Table 1. Details of genotyping methods for six SNPs in *RFC*, *GGH* and *MTHFR*

Genes	SNPs	Methods[a]	Primers[b]	Annealing temperatures	Digestion enzymes	Digestion temperatures	Ref.
RFC	G80A	PCR–RFLP	F: 5′- AGT GTC ACC TTC GTC CCC TC -3′ R: 5′- CTC CCG CGT GAA GTT CTT -3′	60 °C	*Hha* I	37 °C	23,26
GGH	C−401T	PCR–RFLP	F: 5′- TAG AAT CCC CTG CCA GCC TCC TCG -3′ R: 5′- TAA GCG GAG ACT CTG GAA ACG ACT -3′	63 °C	*Bsl* I	55 °C	20 (Modified)
	G−354T	PCR–RFLP	F: 5′- TAG AAT CCC CTG CCA GCC TCC TCG -3′ R: 5′- TAA GCG GAG ACT CTG GAA ACG ACT -3′	63 °C	*Afl* II	37 °C	20 (Modified)
	C452T	PCR–RFLP	F: 5′- GTG CCT ATT TGG TTA TGA CA -3′ R: 5′- CTA CTT ACT AAT CCT GCC CA -3′	55 °C	*Ase* I	37 °C	20,22
MTHFR	C677T	PCR–RFLP	F: 5′- TGA ACA GGT GGA GGC CAG CCT CT -3′ R: 5′- AGG ACG GTG CGG TGA GAG TG -3′	65 °C	*Hinf* I	37 °C	38
	A1298C	AS-PCR	F: 5′- GGA GGA GCT GAC CAG TGA ATA-3′ (for A allele) F: 5′- GGA GGA GCT GAC CAG TGA ATC -3′ (for C allele) R: 5′- CCA CTC CAG CAT CAC TCA CT -3′	55 °C			38 (Modified)

[a]PCR–RFLP and AS-PCR are the abbreviations of polymerase chain reaction–restriction fragment length polymorphism and allele-specific PCR assay, respectively.
[b]F and R are the abbreviations of forward primer and reverse primer, respectively.

weight, creatinine clearance, MTX dose, glucocorticoids dose, and six SNPs of genes coding for three enzymes involved in the folate pathways. CRP-AUC was logarithmically transformed because it had a left-skewed distribution. Factors significantly associated with CRP-AUC in a univariate analysis were included in a multivariate model and a multiple linear regression was used to adjust for the effects of the factors. To evaluate the effects of the combination of the SNPs, the main effect and first-order interaction effect terms of the SNPs were included in the regression models. In statistics, the 'main effect' term is used in the model when one factor is independent of the effect of the other factors, whereas the 'interaction effect' is used when the effects of two or more factors are not simply additive. Such a term implies that the effect of one factor depends on the values of one or more other factors. $P < 0{\cdot}05$ was considered statistically significant. Reported values of P were two-sided. The statistical analyses were performed using R version 2.6.1 (http://www.r-project.org/).

RESULTS

Patient characteristics and genotypes

Eighty-seven Japanese patients with RA met the eligibility criteria (Table 2). The frequencies of the polymorphisms were in Hardy–Weinberg equilibrium.

Effect of each factor on CRP-AUC

In the univariate analysis (Table 3) sex, age and glucocorticoid dose were found to be significantly associated with the CRP-AUC. The results of univariate analysis on the effects of the combination of SNPs are shown in Table 4. The main effect of *RFC* 80GA and AA (vs. GG) was found to be significant; the interaction effects between *RFC* 80AA and *GGH* −401CT/TT (vs. CC) and between RFC 80AA and MTHFR 677CT had values of $P < 0{\cdot}1$. All other main and interaction effects had a value of $P > 0{\cdot}1$. The results of multivariate analysis are shown in Table 5. Age ($P = 0{\cdot}0495$), MTX dose ($P = 0{\cdot}0205$), the effects of *RFC* 80AA ($P = 0{\cdot}0243$) and *GGH* −401 CT/TT ($P = 0{\cdot}0129$), and interaction effect between *RFC* 80AA and *GGH* −401 CT/TT ($P = 0{\cdot}0017$) were significant. The interaction effects between *RFC*

Table 2. Characteristics and genetic polymorphisms of 87 Japanese patients with RA

Age (years)	66 (35–89)
Sex Male/Female (*n*, %)	13/74 (15/85)
Body weight (kg)	47·0 (29·6–80·0)
Creatinine clearance (mL/min)	64·8 (23·9–119·5)
Methotrexate dose (mg/week)	6·0 (2·0–13·3)
Glucocorticoids dose (equivalent to prednisolone, mg/day)	3·8 (0–10·0)
CRP-AUC (mg·1 year/dL)	256 (37–2638)
RFC G80A	
Genotype GG/GA/AA (*n*, %)	21/35/31 (24/40/36)
Allele G/A (*n*, %)	77/97 (44/56)
GGH C–401T	
Genotype CC/CT/TT (*n*, %)	52/32/3 (60/37/3)
Allele C/T (*n*, %)	136/38 (78/22)
GGH G–354T	
Genotype GG/GT/TT (*n*, %)	73/13/1 (84/15/1)
Allele G/T (*n*, %)	159/15 (91/9)
GGH C452T	
Genotype CC/CT/TT (*n*, %)	78/9/0 (90/10/0)
Allele C/T (*n*, %)	165/9 (95/5)
MTHFR C677T	
Genotype CC/CT/TT (*n*, %)	32/40/15 (37/46/17)
Allele C/T (*n*, %)	104/70 (60/40)
MTHFR A1298C	
Genotype AA/AC/CC (*n*, %)	47/32/8 (54/37/9)
Allele A/C (*n*, %)	126/48 (72/28)

Values are median (range) except for sex, genotypes and alleles.

Table 3. Results of univariate analysis of patient characteristics

Factors	Estimate of regression parameters	*P*
Sex (Male vs. Female)	0·7949	0·0283
Age	0·2647	0·0132
Body weight	0·0670	0·5370
Creatinine clearance	−0·0918	0·3980
Methotrexate dose	0·1855	0·0855
Glucocorticoids dose	0·2509	0·0191

80AA and *GGH* −401 CT/TT are shown in the interaction plot (Fig. 1). It can be seen that the effect of *RFC* 80 genotype for *GGH* 401CC is different to those for *GGH* −401CT/TT (Fig. 1). This suggests that patients with RA having *RFC* 80A and *GGH* −401T alleles were less responsive to MTX than those with *RFC* 80A and without *GGH* −401T alleles.

Table 4. Results of univariate analysis on effects of combination of SNPs

Main and interaction effects of SNPs	Estimate of regression parameter	*P*
RFC 80GA	−2·3820	0·0449
RFC 80AA	−2·7844	0·0188
GGH −401CT/TT	−1·4124	0·1792
GGH −354GT/TT	0·1066	0·9524
GGH 452CT	−0·0984	0·9624
MTHFR 677CT	−0·9377	0·3787
MTHFR 677TT	−0·2619	0·8386
MTHFR 1298AC/CC	0·0578	0·9532
RFC 80GA : *GGH* −401CT/TT	0·9712	0·2748
RFC 80AA : *GGH* −401CT/TT	2·2920	0·0239
RFC 80GA : *GGH* −354GT/TT	0·4324	0·7740
RFC 80AA : *GGH* −354GT/TT	0·4975	0·6739
RFC 80GA : *GGH* 452CT	0·1500	0·9239
RFC 80AA : *GGH* 452CT	−0·4757	0·7901
RFC 80GA : *MTHFR* 677CT	1·4738	0·1331
RFC 80AA : *MTHFR* 677CT	1·7264	0·0877
RFC 80GA : *MTHFR* 677TT	0·8753	0·5173
RFC 80AA : *MTHFR* 677TT	−1·3090	0·6004
RFC 80GA : *MTHFR* 1298AC/CC	0·6312	0·5139
RFC 80AA : *MTHFR* 1298AC/CC	0·7240	0·4290
GGH −401CT/TT : *GGH* −354GT/TT	0·3925	0·8322
GGH −401CT/TT : *MTHFR* 677CT	0·2093	0·7864
GGH −401CT/TT : *MTHFR* 677TT	−0·0668	0·9539
GGH −401CT/TT : *MTHFR* 1298AC/CC	−0·4508	0·5602
GGH −354GT/TT : *GGH* 452CT	0·3448	0·8963
GGH −354GT/TT : *MTHFR* 677CT	0·0263	0·9840
GGH −354GT/TT : *MTHFR* 677TT	1·2248	0·5950
GGH −354GT/TT : *MTHFR* 1298AC/CC	−0·3748	0·7484

The colon (:) denotes an interaction effect term. There was no other combination of SNPs.

DISCUSSION

Methotrexate is one of the most widely used anti-cancer and anti-inflammatory agents. Low-dose MTX administered orally as a weekly pulse, has been used extensively in RA therapy (1, 6). It has been reported that SNPs in genes of folate metabolic pathway enzymes affect the efficacy and

Table 5. Results of multivariate analysis

Factors	Estimate of regression parameter	*P*
Sex (Male vs. Female)	0·3990	0·2858
Age	0·0216	0·0495*
Methotrexate dose	0·1431	0·0205*
Glucocorticoids dose	0·0603	0·3083
RFC 80GA	−1·2527	0·0906
RFC 80AA	−1·7036	0·0243*
GGH −401CT/TT	−1·6594	0·0129*
MTHFR 677CT	−0·4829	0·5036
MTHFR 677TT	0·1437	0·8656
RFC 80GA : *GGH* −401CT/TT	0·8156	0·2066
RFC 80AA : *GGH* −401CT/TT	2·1194	0·0017*
RFC 80GA : *MTHFR* 677CT	0·2300	0·7834
RFC 80AA : *MTHFR* 677CT	0·7300	0·3772
RFC 80GA : *MTHFR* 677TT	0·0561	0·9522
RFC 80AA : *MTHFR* 677TT	0·5917	0·6083
GGH −401CT/TT : *MTHFR* 677CT	0·6842	0·2473
GGH −401CT/TT : *MTHFR* 677TT	0·3992	0·5889

The colon (:) denotes an interaction effect term.
*Significance of ($P < 0·05$).

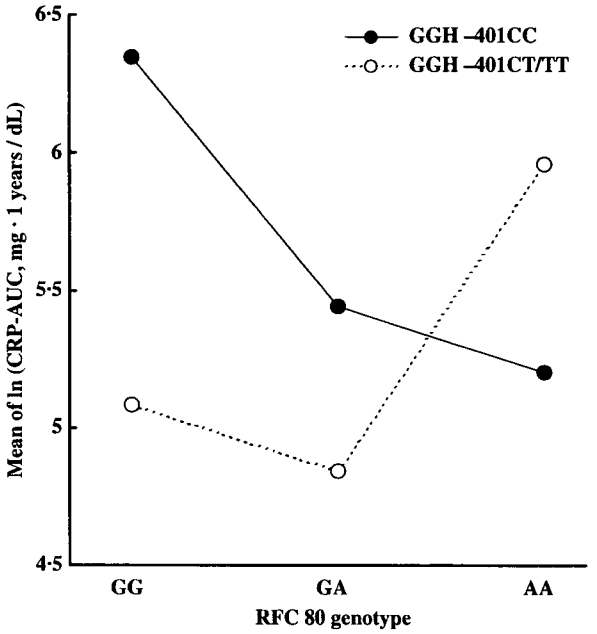

Fig. 1. Interaction plot showing the effects of GGH C-401T genotype and RFC G80A genotype on the mean of the natural logarithm of CRP-AUC in patients with RA receiving low-dose, weekly pulse of MTX. The closed symbol denotes GGH-401CT/TT genotype, whereas the open symbol denotes GGH-401CC genotype.

toxicity of MTX (12, 21, 23–25); however, there are only few reports on the relationship between the interaction effect of these SNPs and MTX efficacy in Japanese patients with RA. Thus, in the present study we evaluated the effects of factors, including the SNPs of folate metabolic pathway enzymes genes such as *RFC*, *GGH* and *MTHFR*, on CRP-AUC, as one of the indices of the anti-inflammatory efficacy of MTX. Our study, suggested that age, MTX dose, the main effects of *RFC* 80AA and *GGH* −401CT/TT genotypes, and the interaction effect between *RFC*80AA and *GGH* −401CT/TT genotypes were significant factors affecting CRP-AUC in patients with RA receiving low-dose MTX. Based on these findings, CRP-AUC would be higher in older patients than in younger patients and, if patients had *RFC* 80AA genotypes, CRP-AUC would be higher in patients with *GGH* −401CT/TT genotypes than in those with the CC genotype.

Previous reports suggest that *RFC* G80A polymorphism is associated with altered MTX plasma level (12). Moreover Molin *et al.* suggested that patients with AA genotype of *RFC* 80 tended to have higher folate polyglutamate levels in blood cells (30). Recent evidence suggests that patients with the *RFC* 80AA genotype responded to therapy better than those with the GG and GA genotypes (13). The results of univariate analysis in our study are consistent with these reports. The *RFC* G80A SNP causing the amino acid change (Arg to His) in the transmembrane domain was expected to alter RFC transport activity (31). Several amino acid changes in a transmembrane domain of RFC in antifolate-resistant cells were shown to change the ratio of RFC affinities to [^{3}H] MTX vs. other folate substrates (32, 33). These reports and our results suggest that the *RFC* 80A allele may potentiate the effect of low-dose MTX in patients with RA. Hence, patients with the *RFC* 80A allele and *GGH* −401CT/TT genotypes were less responsive to MTX than those without *GGH* −401T alleles in the present study.

Chave *et al.* indicated that a *GGH* C−401T polymorphism in the *GGH* promoter region was associated with increased luciferase activity and hypothesized that the polymorphism may result in increased GGH activity, followed by the

deconjugation of MTX-PGs (20). However, if GGH activity was increased by C–401T polymorphism, the anti-DHFR effect would not be increased even if the MTX concentrations in the cells were higher. Some investigators have advocated routine monitoring of MTX-PGs in red blood cells for management of RA (34–37). Dervieux *et al.* reported that there was an inverse association between *RFC* 80AA and *GGH* –401TT homozygosity and intracellular MTX-PGs concentrations (23); this finding is in good agreement with our results. In our study, 36%, 40%, and 15% of the RA patients were carriers of *RFC* 80AA, *GGH* –401CT/TT and of both *RFC* 80AA and *GGH* –401CT/TT, respectively.

There was no relationship between *GGH* C452T SNP and CRP-AUC in our study. The *GGH* C452T located in exon 5 of the *GGH* gene involving Thr to Ile amino acid exchange resulted in decreased catalytic activity of GGH (21). The allele frequency of *GGH* 452T in a Japanese population is only 5·6% (22). We speculate that there was no statistical relationship between *GGH* C452T and inflammatory status because of low allele frequency. In our study, there was no relationship between *MTHFR* SNPs and CRP-AUC, but Urano *et al.* reported that patients with RA having the MTHFR 677C-1298C haplotype received lower doses of MTX and responded better to treatment than those without it (25). Thus, MTHFR is an important enzyme in the folate metabolic pathway.

In conclusion, we found that the SNPs combination, *RFC* G80A and *GGH* C–401T, could be promising for monitoring anti-inflammatory status in MTX-treated patients with RA, and could be considered as a possible marker for drug response against MTX. Larger confirmatory prospective studies would be valuable.

ACKNOWLEDGEMENTS

We thank Dr Osamu Kimoto, Ms. Chiharu Kuroda and the professional nurses at Shizuoka Kosei Hospital for their medical expertise, and Mr Naoto Harada, University of Shizuoka for his technical support.

REFERENCES

1. Andersen PA, West SG, O'Dell JR, Via CS, Claypool RG, Kotzin BL (1985) Weekly pulse methotrexate in rheumatoid arthritis. Clinical and immunologic effects in a randomized, double-blind study. *Annals of Internal Medicine*, **103**, 489–496.
2. Evans WE, Relling MV, Rodman JH, Crom WR, Boyett JM, Pui CH (1998) Conventional compared with individualized chemotherapy for childhood acute lymphoblastic leukemia. *The New England Journal of Medicine*, **338**, 499–505.
3. Gorlick R, Goker E, Trippett T, Waltham M, Banerjee D, Bertino JR (1996) Intrinsic and acquired resistance to methotrexate in acute leukemia. *The New England Journal of Medicine*, **335**, 1041–1948.
4. Pui CH, Campana D, Evans WE (2001) Childhood acute lymphoblastic leukaemia – current status and future perspectives. *The Lancet Oncology*, **2**, 597–607.
5. Pui CH, Evans WE (1998) Acute lymphoblastic leukemia. *The New England Journal of Medicine*, **339**, 605–615.
6. Weinblatt ME, Coblyn JS, Fox DA *et al.* (1985) Efficacy of low-dose methotrexate in rheumatoid arthritis. *The New England Journal of Medicine*, **312**, 818–822.
7. American College of Rheumatology Subcommittee on Rheumatoid Arthritis Guidelines. (2002) Guidelines for the management of rheumatoid arthritis: 2002 Update. *Arthritis and Rheumatism*, **46**, 328–346.
8. van Ede AE, Laan RF, Blom HJ, De Abreu RA, van de Putte LB (1998) Methotrexate in rheumatoid arthritis: an update with focus on mechanisms involved in toxicity. *Seminars in arthritis and rheumatism*, **27**, 277–292.
9. Bathon JM, Martin RW, Fleischmann RM *et al.* (2000) A comparison of etanercept and methotrexate in patients with early rheumatoid arthritis. *The New England Journal of Medicine*, **343**, 1586–1593.
10. Seideman P (1993) Methotrexate – the relationship between dose and clinical effect. *British Journal of Rheumatology*, **32**, 751–753.
11. Strand V, Cohen S, Schiff M *et al.* (1999) Treatment of active rheumatoid arthritis with leflunomide compared with placebo and methotrexate. Leflunomide Rheumatoid Arthritis Investigators Group. *Archives of Internal Medicine*, **159**, 2542–2550.
12. Laverdiere C, Chiasson S, Costea I, Moghrabi A, Krajinovic M (2002) Polymorphism G80A in the reduced folate carrier gene and its relationship to methotrexate plasma levels and outcome of childhood acute lymphoblastic leukemia. *Blood*, **100**, 3832–3834.
13. Drozdzik M, Rudas T, Pawlik A, Gornik W, Kurzawski M, Herczynska M (2007) Reduced folate carrier-1 80G>A polymorphism affects methotrexate treatment outcome in rheumatoid arthritis. *The Pharmacogenomics Journal*, **7**, 404–407.
14. Goldman ID, Lichtenstein NS, Oliverio VT (1968) Carrier-mediated transport of the folic acid analogue, methotrexate, in the L1210 leukemia cell. *Journal of Biological Chemistry*, **243**, 5007–5017.

15. Shane B (1989) Folylpolyglutamate synthesis and role in the regulation of one-carbon metabolism. *Vitamins and Hormones*, **45**, 263–335.
16. Zhao R, Goldman ID (2003) Resistance to antifolates. *Oncogene*, **22**, 7431–7457.
17. Rots MG, Pieters R, Kaspers GJ, Veerman AJ, Peters GJ, Jansen G (2000) Classification of ex vivo methotrexate resistance in acute lymphoblastic and myeloid leukaemia. *British Journal of Haematology*, **110**, 791–800.
18. Panetta JC, Wall A, Pui CH, Relling MV, Evans WE (2002) Methotrexate intracellular disposition in acute lymphoblastic leukemia: a mathematical model of gamma-glutamyl hydrolase activity. *Clinical Cancer Research*, **8**, 2423–2429.
19. Rhee MS, Lindau-Shepard B, Chave KJ, Galivan J, Ryan TJ (1998) Characterization of human cellular gamma-glutamyl hydrolase. *Molecular Pharmacology*, **53**, 1040–1046.
20. Chave KJ, Ryan TJ, Chmura SE, Galivan J (2003) Identification of single nucleotide polymorphisms in the human gamma-glutamyl hydrolase gene and characterization of promoter polymorphisms. *Gene*, **319**, 167–175.
21. Cheng Q, Wu B, Kager L *et al.* (2004) A substrate specific functional polymorphism of human gamma-glutamyl hydrolase alters catalytic activity and methotrexate polyglutamate accumulation in acute lymphoblastic leukaemia cells. *Pharmacogenetics*, **14**, 557–567.
22. Hayashi H, Fujimaki C, Inoue K, Suzuki T, Itoh K (2007) Genetic polymorphism of C452T (T127I) in human gamma-glutamyl hydrolase in a Japanese population. *Biological and Pharmaceutical Bulletin*, **30**, 839–841.
23. Dervieux T, Kremer J, Lein DO *et al.* (2004) Contribution of common polymorphisms in reduced folate carrier and gamma-glutamylhydrolase to methotrexate polyglutamate levels in patients with rheumatoid arthritis. *Pharmacogenetics*, **14**, 733–739.
24. Ulrich CM, Yasui Y, Storb R *et al.* (2001) Pharmacogenetics of methotrexate: toxicity among marrow transplantation patients varies with the methylenetetrahydrofolate reductase C677T polymorphism. *Blood*, **98**, 231–234.
25. Urano W, Taniguchi A, Yamanaka H *et al.* (2002) Polymorphisms in the methylenetetrahydrofolate reductase gene were associated with both the efficacy and the toxicity of methotrexate used for the treatment of rheumatoid arthritis, as evidenced by single locus and haplotype analyses. *Pharmacogenetics*, **12**, 183–190.
26. Hassell AB, Davis MJ, Fowler PD *et al.* (1993) The relationship between serial measures of disease activity and outcome in rheumatoid arthritis. *The Quarterly Journal of Medicine*, **86**, 601–607.
27. Plant MJ, Williams AL, O'Sullivan MM, Lewis PA, Coles EC, Jessop JD (2000) Relationship between time-integrated C-reactive protein levels and radiologic progression in patients with rheumatoid arthritis. *Arthritis and Rheumatism*, **43**, 1473–1477.
28. Cockcroft DW, Gault MH (1976) Prediction of creatinine clearance from serum creatinine. *Nephron*, **16**, 31–41.
29. Souverein PC, Berard A, Van Staa TP *et al.* (2004) Use of oral glucocorticoids and risk of cardiovascular and cerebrovascular disease in a population based case-control study. *Heart*, **90**, 859–865.
30. Morin I, Devlin AM, Leclerc D *et al.* (2003) Evaluation of genetic variants in the reduced folate carrier and in glutamate carboxypeptidase II for spina bifida risk. *Molecular Genetics and Metabolism.*, **79**, 197–200.
31. Whetstine JR, Gifford AJ, Witt T *et al.* (2001) Single nucleotide polymorphisms in the human reduced folate carrier: characterization of a high-frequency G/A variant at position 80 and transport properties of the His(27) and Arg(27) carriers. *Clinical Cancer Research*, **7**, 3416–3422.
32. Drori S, Jansen G, Mauritz R, Peters GJ, Assaraf YG (2000) Clustering of mutations in the first transmembrane domain of the human reduced folate carrier in GW1843U89-resistant leukemia cells with impaired antifolate transport and augmented folate uptake. *The Journal of Biological Chemistry*, **275**, 30855–30863.
33. Jansen G, Mauritz R, Drori S *et al.* (1998) A structurally altered human reduced folate carrier with increased folic acid transport mediates a novel mechanism of antifolate resistance. *The Journal of Biological Chemistry*, **273**, 30189–30198.
34. Dervieux T, Orentas Lein D, Marcelletti J *et al.* (2003) HPLC determination of erythrocyte methotrexate polyglutamates after low-dose methotrexate therapy in patients with rheumatoid arthritis. *Clinical Chemistry*, **49**, 1632–1641.
35. Kamen BA, Takach PL, Vatev R, Caston JD (1976) A rapid, radiochemical-ligand binding assay for methotrexate. *Analytical Biochemistry*, **70**, 54–63.
36. Kamen BA, Winick N (1986) Analysis of methotrexate polyglutamate derivatives *in vivo*. *Methods in Enzymology*, **122**, 339–346.
37. Schroder H, Heinsvig EM (1985) Enzymatic assay for methotrexate in erythrocytes. *Scandinavian Journal of Clinical and Laboratory Investigation*, **45**, 657–659.
38. Yi P, Pogribny I, Jill James S (2002) Multiplex PCR for simultaneous detection of 677 C → T and 1298 A → C polymorphisms in methylenetetrahydrofolate reductase gene for population studies of cancer risk. *Cancer Letters*, **181**, 209–213.

The KK-Periome Database for Transcripts of Periodontal Ligament Development

MASAHIRO SAITO[1]*, EISAKU NISHIDA[1], TAKASHI SASAKI[2,3], TOSHIYUKI YONEDA[1], AND NOBUYOSHI SHIMIZU[3]
[1]*Department of Molecular and Cellular Biochemistry, Osaka University Graduate School of Dentistry, Osaka, Japan*
[2]*Department of Molecular Biology, Keio University School of Medicine, Tokyo, Japan*
[3]*Advanced Research Center for Genome Super Power, Keio University, Tsukuba, Japan*

ABSTRACT The periodontal ligament (PDL) is a strong connective tissue that surrounds the tooth root, absorbs occlusal forces, and functions as a sense organ. PDL originated from dental follicle (DF), which possessed mesenchymal progenitors in the developing tooth germ. However, as specific marker genes for PDL and DF are currently unavailable, the molecular mechanisms of PDL development are yet to be clarified. To facilitate the identification of such genes, we have previously established a transcriptome database of the human PDL (the KK-Periome database) and screened for specific genes expressed during PDL development. Initial screening of the database revealed two marker genes for distinguishing DF and PDL. The KK-Periome database thus appears to offer a useful resource for investigating genes involved in PDL development. *J. Exp. Zool. (Mol. Dev. Evol.) 312B, 2009.* © 2009 Wiley-Liss, Inc.

How to cite this article: Saito M, Nishida E, Sasaki T, Yoneda T, Shimizu N. 2009. The KK-Periome database for transcripts of periodontal ligament development. J. Exp. Zool. (Mol. Dev. Evol.) 312B:[page range].

The periodontium is a tooth-supporting tissue comprising gingiva, periodontal ligament (PDL), cementum, and alveolar bone (Ten Cate, '94). More specifically, the PDL is an element that connects the cementum covering the tooth root surface and the alveolar bone of the maxilla or mandible (Ten Cate and Mills, '72; Beertsen et al., '97; McCulloch et al., 2000). The PDL has the ability to absorb mechanical stress, and has thus been compared with tendon and ligament (McCulloch et al., 2000; Yoshizawa et al., 2004). Similar to tendons and ligaments, collagen type I is predominant, although other types of collagen (types III, V, VI, and XII) and proteoglycans that regulate collagen fibril formation are also deposited in the PDL (Lukinmaa and Waltimo, '92; Liu et al., '95; Everts et al., '98; MacNeil et al., '98). PDL cells also express genes involved in tendon and ligament formation, such as scleraxis and growth and differentiation factors-5, -6, and -7 (Sena et al., 2003; Seo et al., 2004; Yokoi et al., 2007). The cellular content of PDL is predominated by PDL cells, which can form Sharpey's fibers, collagen fibers embedded into the calcified matrix (McCulloch et al., 2000; Nanci and Bosshardt, 2006). Previous findings have suggested that although cultured PDL cells fail to form mineralized nodules, a partial resemblance to osteoblasts is apparent, such as high alkaline phosphatase activity and expression of osteoblast marker genes including RUNX2, bone sialoprotein, and type I collagen (Yamashita et al., '87; Nojima et al., '90; Lekic et al., 2001; Saito et al., 2002; Murakami et al., 2003). Recently, regulatory mechanisms preventing osteoblastic differentiation have been identified in cultured PDL cells, suggesting that the ability for suppressing osteoblast function may

Grant sponsor: Ministry of Education, Culture, Sports, Science and Technology (MEXT).
*Correspondence to: Masahiro Saito, Department of Molecular and Cellular Biochemistry, Osaka University Graduate School of Dentistry, 1–8 Yamadaoka, Suita, Osaka 565-0871, Japan.
E-mail: mssaito@dent.osaka-u.ac.jp
Received 13 November 2008; Accepted 14 November 2008
Published online in Wiley InterScience (www.interscience.wiley.com). DOI: 10.1002/jez.b.21257

act to prevent PDL from mineralizing (Yoshizawa et al., 2004; Yamada et al., 2007).

The structure of the PDL is often irreversibly damaged when chronic inflammation in the form of "periodontitis" develops, suppressing the periodontium (Bartold and Narayanan, 2006). Although various treatments are available for periodontitis, reliable regeneration of the PDL is not yet possible (Melcher et al., '86; Somerman et al., '99; Bartold et al., 2000; Shimono et al., 2003). A basic understanding of PDL development at the molecular level is required to develop regeneration therapy of PDL, as the regeneration process needs to mimic the cellular events of PDL development (Grzesik and Narayanan, 2002). Recent advances have revealed the existence of progenitor or stem cells in adult PDL (Handa et al., 2002a; Seo et al., 2004; Fujii et al., 2008). To clarify the differentiation mechanisms of these cells, it is necessary to investigate the molecular basis of PDL development.

Progenitor cells are generated by multipotent stem cells and can differentiate into one specific type of cell depending on the cellular environment during organogenesis (Potten and Loeffler, '90). In the case of PDL development, dental mesenchyme generates the dental follicle (DF), which contains PDL cell progenitors that contribute to the formation of the PDL (Cho and Garant, 2000). However, the molecular aspects of PDL development are only vaguely understood owing to the limited information available on marker genes for PDL cell progenitors and PDL cells. Conversely, thanks to recent advances in the availability of genome sequence information for both human and mouse, transcriptomes for various tissues, and bioinformatics for database construction, the identification of genes potentially involved in the development of specialized tissues has become possible (Sunkin and Hohmann, 2007). We describe herein the initial screening of potential marker genes for PDL cell progenitor and PDL cells from the KK-Periome database, which is a collection of transcripts expressed during human PDL development. The significance of extracellular matrix (ECM) components as markers for PDL development is discussed.

MOLECULAR MECHANISMS OF PDL DEVELOPMENT

The PDL originates from the DF formed during the cap stage of tooth germ development by an ectomesenchymal progenitor cell population originating from cranial neural crest cells (Chai et al., 2000; Cho and Garant, 2000). DF is formed from cranial neural crest-derived dental mesenchyme on embryonic day 15 (E15) mouse embryo at the stage of tooth germ development (Fig. 1). As DF contains three kinds of progenitor cells (cementoblast, PDL cell, and osteoblast progenitors), developmental events in the DF are of considerable interest (Morotome et al., '98; Hou et al., '99; Saito et al., 2005). At the cap stage in E15 mouse embryo, dental mesenchyme undergoes differentiation into two distinct types of cells: dental papilla (DP) cells and DF cells (Chai et al., 2000; Cho and Garant, 2000). At the E17 bell

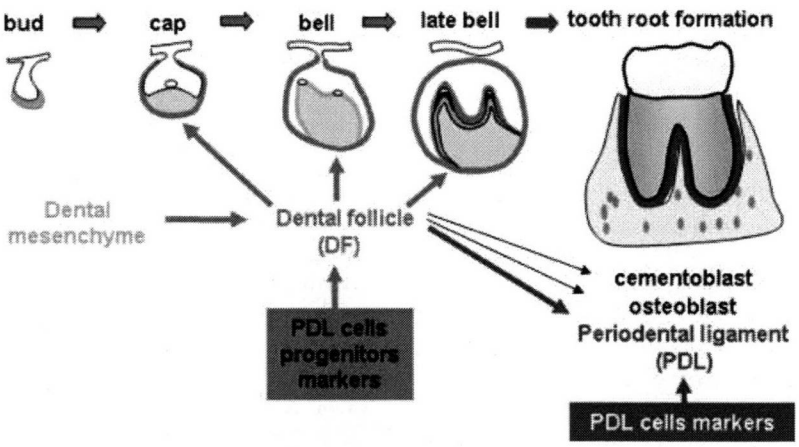

Fig. 1. Schematic of periodontal ligament development. The dental follicle (DF) is initially formed from dental mesenchyme in the cap stage of tooth germ, and differentiates to progenitors of the periodontal ligament (PDL), cementoblasts, and osteoblasts during the bell and late bell stages. After birth, differentiation of progenitors within the DF forms periodontium during the tooth root formation stage. Investigation of the molecular mechanisms underlying the PDL development requires the identification of specific marker for PDL cell progenitors and PDL cells.

stage, DP cells differentiate into cells of the odontogenic lineage, such as odontoblasts or dental pulp cells, eventually giving rise to the dentin–pulp complex in the tooth (Thesleff et al., 2001). After birth, differentiation begins during tooth root formation when cementoblast progenitors migrate to the surface of the tooth root and differentiate into cementoblasts to form cementum matrix (Bosshardt and Schroeder, '96; Saito et al., 2001). At almost the same time, PDL progenitors differentiate into PDL on cementoblasts, inserting collagen fibers known as Sharpey's fibers into the cementum matrix. Fiber insertion also takes place along the alveolar bone. Finally, both bone- and PDL-derived fibers coalesce in the PDL to form the intermediate plexus, which resembles tendinous tissue (Johnson, '87; Cho and Garant, '89, '96).

The fate of progenitor cells in the DF has been investigated using cultured DF cells. Because the experimental model for in vitro differentiation of PDL is not available, implantation analysis using immunodeficiency mice has been used for studying the potential of PDL formation. For instance, cultured DF cells do not form mineralized nodules in vitro even after treatment with mineralization-inducing medium, but are able to form PDL-like tissue and cementum-like structures after implantation into immunodeficient mice (Handa et al., 2002b; Yokoi et al., 2007). In addition, progenitor cell lines for cementoblasts and PDL have been established from immortalized DF cells using single cell cloning methods (Morsczeck et al., 2005; Saito et al., 2005; Luan et al., 2006). These findings support the notion that PDL cell progenitors are present in DF. Investigation of the differentiation of PDL cell progenitors into PDL has thus enabled clarification of transcription factors, signaling molecules, and specific niches involved in PDL differentiation. However, elucidation of the precise differentiation mechanisms for PDL cell progenitors in DF has been hampered by the paucity of specific marker genes for these cells (Pitaru et al., '94; Diekwisch, 2002; Nanci and Bosshardt, 2006). Identification of specific markers that can distinguish PDL cell progenitors and PDL cells is thus important (Fig. 1).

FUNCTIONAL MOLECULES INVOLVED IN PDL DEVELOPMENT

Although no specific marker for PDL is available, several reports have shown that PDL development seems to be dependent on the ECM, which regulates collagen fibril formation and is mainly deposited in PDL (McCulloch, 2000). Type I and III collagens are the major components of collagen bundles and Sharpey's fibers in PDL, and fibril assembly is responsible for the structural stabilization and mechanical characteristics of the PDL (Ten Cate, '94; MacNeil et al., '98). Interactions between fibrillar collagen and small leucine-rich proteoglycans (SLRPs) such as lumican and decorin regulate flexible connective tissues such as tendons (Danielson et al., '97; Ezura et al., 2000; Matheson et al., 2005). Lumican- and decorin-deficient mice show abnormal collagen fibrils in PDL, indicating that these SLRPs regulate the organization of collagen fibrils during PDL formation (Matheson et al., 2005). Conversely, Yamada et al. (2001, 2007) found that PDL-associated protein (PLAP)-1/asporin, which belongs to a novel SLRP family, is specifically expressed not only in DF but also in adult PDL. PLAP-1/asporin directly interacts with bone morphogenetic protein-2 to inhibit the mineralization of the PDL. This finding strongly suggests that PDL synthesizes PLAP-1/asporin as a negative regulator of mineralization to prevent ankylosis. Noncollagenous ECM is also involved in the formation of PDL. Periostin is a secreted adhesion protein that displays homology with fasciclin I, an insect growth cone guidance protein (Horiuchi et al., '99). During tooth germ development, periostin is initially expressed in the DF, and then becomes restricted to postnatal PDL during tooth root formation (Kruzynska-Frejtag et al., 2004). Periostin-deficient mice show disorganization of the PDL and alveolar bone resorption, suggesting a critical role of this protein in the maintenance of PDL and onset of periodontal disease (Rios et al., 2005; Kii et al., 2006).

As PDL is morphologically similar to tendon and ligament, the suggestion has been made that tendon/ligament phenotype-related genes that are specifically expressed during the formation of tendons and ligaments are involved in the differentiation of PDL cell progenitors (Table 1) (Oliver et al., '95; Wolfman et al., '97; Brent et al., 2003; Salingcarnboriboon et al., 2003). Based on these observations, the ECM predominantly deposited in PDL and tendon/ligament-related genes that are expressed in PDL may contribute to the formation of PDL. However, it is difficult to investigate whether these factors are involved in PDL development owing to the lack of specific markers for PDL cell progenitors and PDL cells.

TABLE 1. List of tendon- and ligament-related genes

Functional categorization	Gene name	References
Transcription factor	Scleraxis	Brent et al. (2003)
	Six1 Six2	Oliver et al. ('95)
Plasma membrane protein	EphA4	Patel et al. ('96)
Signaling molecules	GDF5	Sodersten et al. (2005) and Wolfman et al. ('97)
	GDF6 GDF7	

Genes expressed in tendon and ligament are listed according to functional categorization. GDF, growth and differentiation factor.

THE KK-PERIOME DATABASE AND SCREENING OF SPECIFIC MARKER FOR PDL CELL PROGENITORS AND PDL CELLS

To identify specific markers for PDL cell progenitors and PDL cells, we established the KK-Periome database as a collection of 617 clusters of expressed sequence tags (ESTs) highly expressed in human PDL (Nishida et al., 2007). These EST clusters were derived from short single-pass sequence reads of 11,520 randomly selected clones from the human PDL cDNA library and were considered invaluable for identifying particular genes and unique gene expression patterns during PDL development. For the identification of specific markers for PDL cell progenitors and PDL cells from the KK-Periome database, screening of candidate genes was performed using two different criteria of functional classification and expression pattern (Fig. 2). As ECM components are considered to be involved in the determination of cell specificity (Engler et al., 2006; Scadden, 2006), we hypothesized that the DF and the PDL are each composed of specific ECM proteins, and that these unique matrices could serve as specific markers for PDL cell progenitors or PDL cells. As a result of functional classification, we obtained 38 ECM clusters from KK-Periome database, which include type I collagen α 2, Secreted proteins acidic, cystein-rich (SPARC)/osteonectin, collagen type III, periostin, lumican, type I collagen α I chain, osteopontin, decorin, fibronectin, and PLAP-1/asporin as the ten most highly expressed transcripts. Most of the ECM proteins present here for the characterization of the PDL are ubiquitous molecules although the PDL has a unique structure and function (Yamada et al., 2001). Therefore, we next screened ECM proteins that had not previously been reported in PDL according to a PubMed search, and 13 ECM clusters were obtained as candidates, including the genes for collagen type XI α 1, SPARC-like 1, tenascin-N, collagen type XV α 1, hyaluronan and proteoglycan link protein 1, vitrin, type XVI collagen α 1, SPARC-related modular calcium binding 2, granulin, fibulin 5, F-spondin, nidogen 1, and leprecan 1. We next investigated temporal and spatial expression patterns of these 13 candidate genes using in situ hybridization analysis with mouse DF and PDL tissues. As a result, two genes

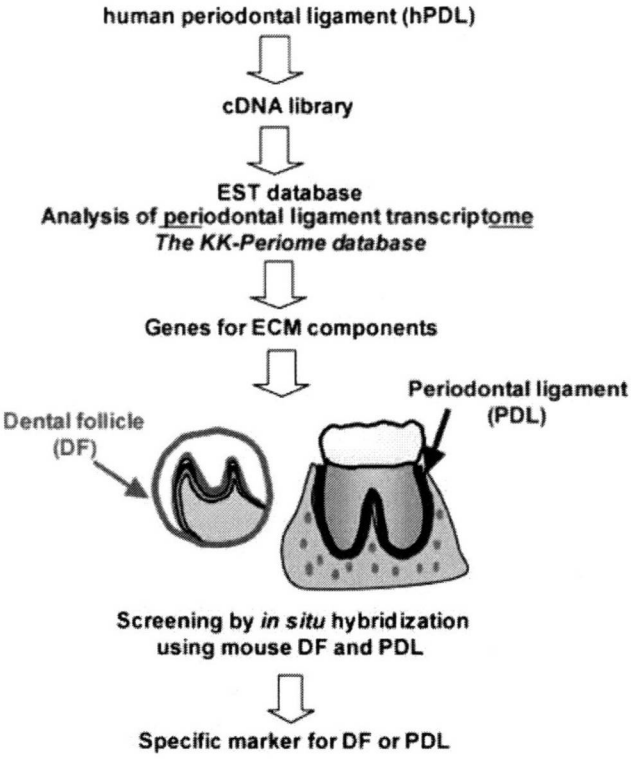

Fig. 2. Strategy for creating a transcriptome database for PDL (KK-Periome database) and a screening marker for PDL cell progenitors and PDL cells. The KK-Periome database was established following the expressed sequence tag (EST) sequence analysis of the human PDL cDNA library. Genes for ECM components including collagen type XI α 1, SPARC-like 1, tenascin-N, collagen type XV α 1, hyaluronan and proteoglycan link protein 1, vitrin, type XVI collagen α 1, SPARC-related modular calcium binding 2, granulin, fibulin 5, F-spondin, nidogen 1, and leprecan 1 were isolated and specific marker for PDL cell progenitors and PDL were screened by in situ hybridization analysis of mouse DF and PDL. PDL, periodontal ligament; ECM, extracellular matrix; DF, dental follicle.

(F-spondin and tenascin-N) were identified as candidate markers for the DF and the PDL, respectively. Interestingly, F-spondin was initially expressed in the DF at the cap stage and became progressively more evident in the DF at the bell stage. In addition, no expression of F-spondin was observed in other types of cells in the tooth germ, including DP, dental epithelium, odontoblasts, or ameloblasts. However, expression of F-spondin in DF was significantly down-regulated after birth and completely absent in the PDL of adult mice. Unlike F-spondin, expression of tenascin-N was not detected in DF cells of the developing tooth germ in the embryo, but was strongly induced in adult PDL. Although PDL contained several types of cells including PDL cells, epithelial cells of Malassez, endothelial cells, osteoblast progenitors, and cementoblast progenitors (McCulloch et al., 2000), the expression of tenascin-N is restricted to adult PDL cells. Based on these observations, F-spondin and tenascin-N may serve as specific markers for DF or PDL, respectively (Fig. 3).

F-SPONDIN AND TENASCIN-N AS MARKERS FOR PDL CELL PROGENITORS AND PDL CELLS

F-spondin is a component of the ECM, which is known to be present in the embryonic floor plate of vertebrates (Klar et al., '92; Tzarfati-Majar et al., 2001) and the caudal somite of birds (Debby-Brafman et al., '99), apparently playing a dual role in the patterning of the nervous system. F-spondin promotes the adhesion and the outgrowth of axons, but inhibits the adhesion of neural crest cells. As F-spondin-knockout mice or transgenic mice expressing F-spondin specifically in PDL are not available, the precise function of F-spondin during PDL development is unclear. However, transient expression of F-spondin in DF strongly suggests the involvement of PDL development, rather than the maintenance of adult PDL function such as withstanding force of mastication. F-spondin was highly expressed in a human cementoblast cell line, and overexpression induced the up-regulation of cementoblast/osteoblast mar-

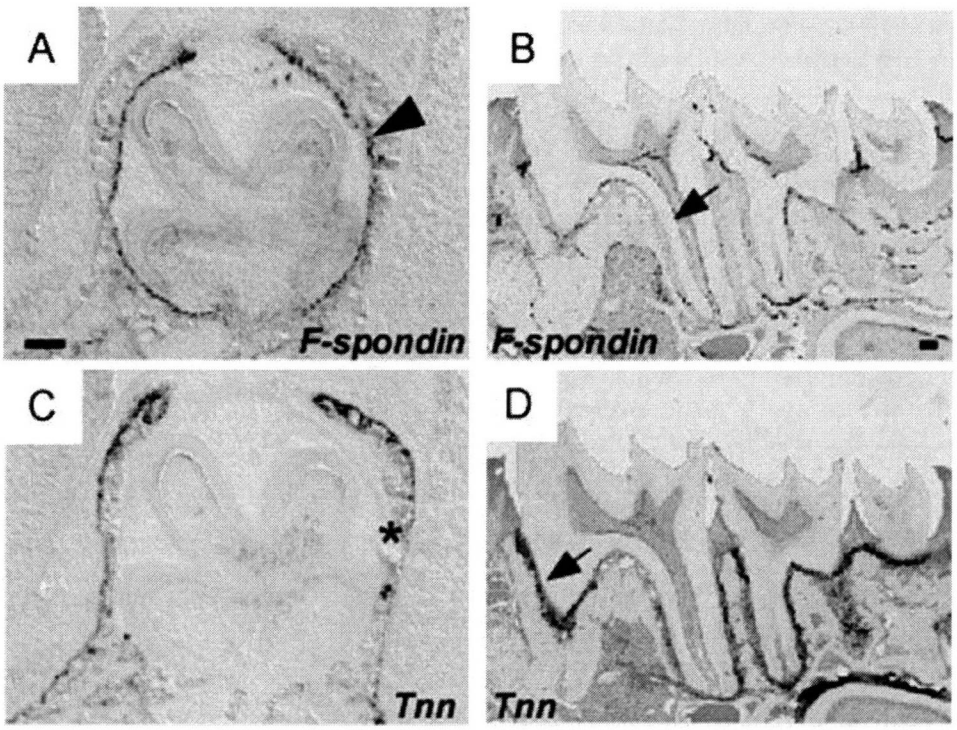

Fig. 3. Expression of F-spondin and tenascin-N during PDL development. In situ hybridization analyses of *F-spondin* (**A** and **B**) and *tenascin-N* (**C** and **D**) in the late bell stage of tooth germ (A and C) and adult molar (B and D) are shown. Note that *F-spondin* is intensely expressed in DF (A, arrowhead), whereas expression is significantly down-regulated in PDL (B, arrow). In contrast, *tenascin-N* (*Tnn*) is strongly expressed in the PDL (D, arrow), but not expressed in the DF (C, asterisk). Bar, 50 μm. Reprinted from Nishida et al. 2007. Transcriptome database KK-Periome for periodontal ligament development: expression profiles of the extracellular matrix genes. Gene 404:70–79 with permission from Elsevier. PDL, periodontal ligament; DF, dental follicle.

ker gene such as bone sialoprotein and osteocalcin (Kitagawa et al., 2006). Moreover, F-spondin protein was detected in the cementum matrix. Contrasting with these results, we found high levels of F-spondin mRNA in the DF and dramatic decreases in the adult PDL suggesting that F-spondin may involve in the formation of DF.

Tenascin-N is a novel member of the tenascin family of proteins, which are expressed in the brain, kidneys, and spleen of adult animals. Unlike other tenascins, tenascin-N is highly expressed in neurons of the central nervous system (Neidhardt et al., 2003). Interestingly, the expression of tenascin-N was strongly up-regulated in the adult PDL, whereas no expression was observed in the DF. Periostin has been used as a marker for distinguishing PDL from adjacent connective tissues such as bone and gingiva in adult tissue (Horiuchi et al., '99; Kruzynska-Frejtag et al., 2004). The expression of periostin was detected in both adult PDL and DF in the developing tooth germ. In contrast to periostin, tenascin-N was specifically expressed in adult PDL (Nishida et al., 2007). In addition, the expression patterning of PLAP-1/asporin resembled that of periostin during PDL development (Yamada et al., 2007). Tenascin-N was thus considered to serve as a distinct marker of differentiated PDL cells. Furthermore, tenascin-N was detected in the costal perichondrocytes that eventually form the ligament tissue suggesting that the expression may be associated with the formation of ligamentous tissues (Nishida et al., 2007).

CONCLUSION

PDL development requires PDL cell progenitors present in the DF during tooth germ development (Cho and Garant, 2000). Although stem/progenitor cells capable of forming PDL have been identified (Seo et al., 2004; Yokoi et al., 2007; Fujii et al., 2008), the precise differentiation mechanisms of these cells remain unclear owing to the unavailability of markers for PDL cell progenitors and PDL cells. A combination of the transcriptome database for the human PDL (KK-Periome database) and in situ hybridization analysis helped to identify F-spondin and tenascin-N as specific markers for PDL cell progenitor or PDL cells, respectively (Fig. 4). Although functional roles of F-spondin and tenascin-N are unclear, development of the PDL is apparently associated with changes in the expression of these proteins. To investigate whether these molecules are involved in PDL formation, development of functional assay system either in vitro or using transgenic mice is necessary. However, further screening of the KK-Periome database may provide more novel marker genes that are useful for analyzing the molecular mechanisms of PDL development and identification of eventual therapeutic targets for the treatment of periodontal disease.

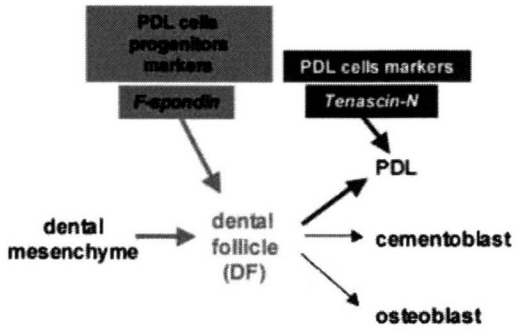

Fig. 4. F-spondin and tenascin-N as markers for PDL cell progenitors or PDL cells. F-spondin is specifically expressed in DF, whereas the expression is significantly down-regulated in PDL. In contrast, expression of tenascin-N is strongly induced in the PDL. We thus proposed F-spondin and tenascin-N as markers for PDL cell progenitors or PDL cells. PDL, periodontal ligament; DF, dental follicle.

ACKNOWLEDGMENTS

We wish to thank all the members of the Department of Molecular and Cellular Biochemistry at the Osaka University School of Dentistry. This work was supported by a Grant-in-Aid for a High-Tech Research Center Project from the Ministry of Education, Culture, Sports, Science and Technology (MEXT) of Japan, the AGU High-Tech Research Center Project, the 2003 Multidisciplinary Research Project from MEXT, and grants from MEXT.

LITERATURE CITED

Bartold P, Narayanan A. 2006. Molecular and cell biology of healthy and diseased periodontal tissues. Periodontol 2000 40:29–49.

Bartold PM, McCulloch CA, Narayanan AS, Pitaru S. 2000. Tissue engineering: a new paradigm for periodontal regeneration based on molecular and cell biology. Periodontol 2000 24:253–269.

Beertsen W, McCulloch CA, Sodek J. 1997. The periodontal ligament: a unique, multifunctional connective tissue. Periodontol 2000 13:20–40.

Bosshardt DD, Schroeder HE. 1996. Cementogenesis reviewed: a comparison between human premolars and rodent molars. Anat Rec 245:267–292.

Brent AE, Schweitzer R, Tabin CJ. 2003. A somitic compartment of tendon progenitors. Cell 113:235–248.

Chai Y, Jiang X, Ito Y, Bringas Jr P, Han J, Rowitch DH, Soriano P, McMahon AP, Sucov HM. 2000. Fate of the mammalian cranial neural crest during tooth and mandibular morphogenesis. Development 127:1671–1679.

Cho MI, Garant PR. 1989. Radioautographic study of [3H]mannose utilization during cementoblast differentiation, formation of acellular cementum, and development of periodontal ligament principal fibers. Anat Rec 223:209–222.

Cho MI, Garant PR. 1996. Expression and role of epidermal growth factor receptors during differentiation of cementoblasts, osteoblasts, and periodontal ligament fibroblasts in the rat. Anat Rec 245:342–360.

Cho MI, Garant PR. 2000. Development and general structure of the periodontium. Periodontol 2000 24:9–27.

Danielson KG, Baribault H, Holmes DF, Graham H, Kadler KE, Iozzo RV. 1997. Targeted disruption of decorin leads to abnormal collagen fibril morphology and skin fragility. J Cell Biol 136:729–743.

Debby-Brafman A, Burstyn-Cohen T, Klar A, Kalcheim C. 1999. F-spondin, expressed in somite regions avoided by neural crest cells, mediates inhibition of distinct somite domains to neural crest migration. Neuron 22: 475–488.

Diekwisch TG. 2002. Pathways and fate of migratory cells during late tooth organogenesis. Connect Tissue Res 43:245–256.

Engler AJ, Sen S, Sweeney HL, Discher DE. 2006. Matrix elasticity directs stem cell lineage specification. Cell 126:677–689.

Everts V, Niehof A, Jansen D, Beertsen W. 1998. Type VI collagen is associated with microfibrils and oxytalan fibers in the extracellular matrix of periodontium, mesenterium and periosteum. J Periodontal Res 33:118–125.

Ezura Y, Chakravarti S, Oldberg A, Chervoneva I, Birk DE. 2000. Differential expression of lumican and fibromodulin regulate collagen fibrillogenesis in developing mouse tendons. J Cell Biol 151:779–788.

Fujii S, Maeda H, Wada N, Tomokiyo A, Saito M, Akamine A. 2008. Investigating a clonal human periodontal ligament progenitor/stem cell line in vitro and in vivo. J Cell Physiol 215:743–749.

Grzesik WJ, Narayanan AS. 2002. Cementum and periodontal wound healing and regeneration. Crit Rev Oral Biol Med 13:474–484.

Handa K, Saito M, Tsunoda A, Yamauchi M, Hattori S, Sato S, Toyoda M, Teranaka T, Narayanan AS. 2002a. Progenitor cells from dental follicle are able to form cementum matrix in vivo. Connect Tissue Res 43:406–408.

Handa K, Saito M, Yamauchi M, Kiyono T, Sato S, Teranaka T, Narayanan AS. 2002b. Cementum matrix formation in vivo by cultured dental follicle cells. Bone 31:606–611.

Horiuchi K, Amizuka N, Takeshita S, Takamatsu H, Katsuura M, Ozawa H, Toyama Y, Bonewald LF, Kudo A. 1999. Identification and characterization of a novel protein, periostin, with restricted expression to periosteum and periodontal ligament and increased expression by transforming growth factor beta. J Bone Miner Res 14:1239–1249.

Hou LT, Liu CM, Chen YJ, Wong MY, Chen KC, Chen J, Thomas HF. 1999. Characterization of dental follicle cells in developing mouse molar. Arch Oral Biol 44: 759–770.

Johnson RB. 1987. A classification of Sharpey's fibers within the alveolar bone of the mouse: a high-voltage electron microscope study. Anat Rec 217:339–347.

Kii I, Amizuka N, Minqi L, Kitajima S, Saga Y, Kudo A. 2006. Periostin is an extracellular matrix protein required for eruption of incisors in mice. Biochem Biophys Res Commun 342:766–772.

Kitagawa M, Kudo Y, Iizuka S, Ogawa I, Abiko Y, Miyauchi M, Takata T. 2006. Effect of F-spondin on cementoblastic differentiation of human periodontal ligament cells. Biochem Biophys Res Commun 349:1050–1056. Epub 2006 September 1051.

Klar A, Baldassare M, Jessell TM. 1992. F-spondin: a gene expressed at high levels in the floor plate encodes a secreted protein that promotes neural cell adhesion and neurite extension. Cell 69:95–110.

Kruzynska-Frejtag A, Wang J, Maeda M, Rogers R, Krug E, Hoffman S, Markwald RR, Conway SJ. 2004. Periostin is expressed within the developing teeth at the sites of epithelial–mesenchymal interaction. Dev Dyn 229:857–868.

Lekic P, Rojas J, Birek C, Tenenbaum H, McCulloch CA. 2001. Phenotypic comparison of periodontal ligament cells in vivo and in vitro. J Periodontal Res 36:71–79.

Liu SH, Yang RS, al-Shaikh R, Lane JM. 1995. Collagen in tendon, ligament, and bone healing. A current review. Clin Orthop Relat Res 318:265–278.

Luan X, Ito Y, Dangaria S, Diekwisch TG. 2006. Dental follicle progenitor cell heterogeneity in the developing mouse periodontium. Stem Cells Dev 15:595–608.

Lukinmaa PL, Waltimo J. 1992. Immunohistochemical localization of types I, V, and VI collagen in human permanent teeth and periodontal ligament. J Dent Res 71:391–397.

MacNeil RL, Berry JE, Strayhorn CL, Shigeyama Y, Somerman MJ. 1998. Expression of type I and XII collagen during development of the periodontal ligament in the mouse. Arch Oral Biol 43:779–787.

Matheson S, Larjava H, Hakkinen L. 2005. Distinctive localization and function for lumican, fibromodulin and decorin to regulate collagen fibril organization in periodontal tissues. J Periodontal Res 40:312–324.

McCulloch CA. 2000. Proteomics for the periodontium: current strategies and future promise. Periodontol 2000 40:173–183.

McCulloch CA, Lekic P, McKee MD. 2000. Role of physical forces in regulating the form and function of the periodontal ligament. Periodontol 2000 24:56–72.

Melcher AH, Cheong T, Cox J, Nemeth E, Shiga A. 1986. Synthesis of cementum-like tissue in vitro by cells cultured from bone: a light and electron microscope study. J Periodontal Res 21:592–612.

Morotome Y, Goseki-Sone M, Ishikawa I, Oida S. 1998. Gene expression of growth and differentiation factors-5, -6, and -7 in developing bovine tooth at the root forming stage (published erratum appears in Biochem Biophys Res Commun 1998 May 29;246(3):925). Biochem Biophys Res Commun 244:85–90.

Morsczeck C, Gotz W, Schierholz J, Zeilhofer F, Kuhn U, Mohl C, Sippel C, Hoffmann KH. 2005. Isolation of precursor cells (PCs) from human dental follicle of wisdom teeth. Matrix Biol 24:155–165. Epub 2005 February 2012.

Murakami Y, Kojima T, Nagasawa T, Kobayashi H, Ishikawa I. 2003. Novel isolation of alkaline phosphatase-positive subpopulation from periodontal ligament fibroblasts. J Periodontol 74:780–786.

Nanci A, Bosshardt DD. 2006. Structure of periodontal tissues in health and disease. Periodontol 2000 40:11–28.

Neidhardt J, Fehr S, Kutsche M, Lohler J, Schachner M. 2003. Tenascin-N: characterization of a novel member of the tenascin family that mediates neurite repulsion from hippocampal explants. Mol Cell Neurosci 23:193–209.

Nishida E, Sasaki T, Ishikawa SK, Kosaka K, Aino M, Noguchi T, Teranaka T, Shimizu N, Saito M. 2007. Transcriptome database KK-Periome for periodontal ligament development: expression profiles of the extracellular matrix genes. Gene 404:70–79. Epub 2007 September 2019.

Nojima N, Kobayashi M, Shionome M, Takahashi N, Suda T, Hasegawa K. 1990. Fibroblastic cells derived from bovine periodontal ligaments have the phenotypes of osteoblasts. J Periodontal Res 25:179–185.

Oliver G, Wehr R, Jenkins NA, Copeland NG, Cheyette BN, Hartenstein V, Zipursky SL, Gruss P. 1995. Homeobox genes and connective tissue patterning. Development 121:693–705.

Pitaru S, McCulloch CA, Narayanan SA. 1994. Cellular origins and differentiation control mechanisms during periodontal development and wound healing. J Periodontal Res 29:81–94.

Potten CS, Loeffler M. 1990. Stem cells: attributes, cycles, spirals, pitfalls and uncertainties. Lessons for and from the crypt. Development 110:1001–1020.

Rios H, Koushik SV, Wang H, Wang J, Zhou HM, Lindsley A, Rogers R, Chen Z, Maeda M, Kruzynska-Frejtag A, Feng JQ, Conway SJ. 2005. Periostin null mice exhibit dwarfism, incisor enamel defects, and an early-onset periodontal disease-like phenotype. Mol Cell Biol 25:11131–11144.

Saito M, Iwase M, Maslan S, Nozaki N, Yamauchi M, Handa K, Takahashi O, Sato S, Kawase T, Teranaka T, Narayanan AS. 2001. Expression of cementum-derived attachment protein in bovine tooth germ during cementogenesis. Bone 29:242–248.

Saito Y, Yoshizawa T, Takizawa F, Ikegame M, Ishibashi O, Okuda K, Hara K, Ishibashi K, Obinata M, Kawashima H. 2002. A cell line with characteristics of the periodontal ligament fibroblasts is negatively regulated for mineralization and Runx2/Cbfa1/Osf2 activity, part of which can be overcome by bone morphogenetic protein-2. J Cell Sci 115:4191–4200.

Saito M, Handa K, Kiyono T, Hattori S, Yokoi T, Tsubakimoto T, Harada H, Noguchi T, Toyoda M, Sato S, Teranaka T. 2005. Immortalization of cementoblast progenitor cells with Bmi-1 and TERT. J Bone Miner Res 20:50–57.

Salingcarnboriboon R, Yoshitake H, Tsuji K, Obinata M, Amagasa T, Nifuji A, Noda M. 2003. Establishment of tendon-derived cell lines exhibiting pluripotent mesenchymal stem cell-like property. Exp Cell Res 287:289–300.

Scadden DT. 2006. The stem-cell niche as an entity of action. Nature 441:1075–1079.

Sena K, Morotome Y, Baba O, Terashima T, Takano Y, Ishikawa I. 2003. Gene expression of growth differentiation factors in the developing periodontium of rat molars. J Dent Res 82:166–171.

Seo BM, Miura M, Gronthos S, Bartold PM, Batouli S, Brahim J, Young M, Robey PG, Wang CY, Shi S. 2004. Investigation of multipotent postnatal stem cells from human periodontal ligament. Lancet 364:149–155.

Shimono M, Ishikawa T, Ishikawa H, Matsuzaki H, Hashimoto S, Muramatsu T, Shima K, Matsuzaka K, Inoue T. 2003. Regulatory mechanisms of periodontal regeneration. Microsc Res Tech 60:491–502.

Somerman MJ, Ouyang HJ, Berry JE, Saygin NE, Strayhorn CL, D'Errico JA, Hullinger T, Giannobile WV. 1999. Evolution of periodontal regeneration: from the roots' point of view. J Periodontal Res 34:420–424.

Sunkin SM, Hohmann JG. 2007. Insights from spatially mapped gene expression in the mouse brain. Hum Mol Genet 16:209–219.

Ten Cate AR. 1994. Development of the periodontium. In: Ten Cate AR, editor. Oral histology, development, structure, and function. St. Louis, MO: Mosby. p 257–275.

Ten Cate AR, Mills C. 1972. The development of the periodontium: the origin of alveolar bone. Anat Rec 173:69–77.

Thesleff I, Keranen S, Jernvall J. 2001. Enamel knots as signaling centers linking tooth morphogenesis and odontoblast differentiation. Adv Dent Res 15:14–18.

Tzarfati-Majar V, Burstyn-Cohen T, Klar A. 2001. F-spondin is a contact-repellent molecule for embryonic motor neurons. Proc Natl Acad Sci USA 98:4722–4727.

Wolfman NM, Hattersley G, Cox K, Celeste AJ, Nelson R, Yamaji N, Dube JL, DiBlasio-Smith E, Nove J, Song JJ, Wozney JM, Rosen V. 1997. Ectopic induction of tendon and ligament in rats by growth and differentiation factors 5, 6, and 7, members of the TGF-beta gene family. J Clin Invest 100:321–330.

Yamada S, Murakami S, Matoba R, Ozawa Y, Yokokoji T, Nakahira Y, Ikezawa K, Takayama S, Matsubara K, Okada H. 2001. Expression profile of active genes in human periodontal ligament and isolation of PLAP-1, a novel SLRP family gene. Gene 275:279–286.

Yamada S, Tomoeda M, Ozawa Y, Yoneda S, Terashima Y, Ikezawa K, Ikegawa S, Saito M, Toyosawa S, Murakami S. 2007. PLAP-1/asporin, a novel negative regulator of periodontal ligament mineralization. J Biol Chem 282:23070–23080.

Yamashita Y, Sato M, Noguchi T. 1987. Alkaline phosphatase in the periodontal ligament of the rabbit and macaque monkey. Arch Oral Biol 32:677–678.

Yokoi T, Saito M, Kiyono T, Iseki S, Kosaka K, Nishida E, Tsubakimoto T, Harada H, Eto K, Noguchi T, Teranaka T. 2007. Establishment of immortalized dental follicle cells for generating periodontal ligament in vivo. Cell Tissue Res 327:301–311.

Yoshizawa T, Takizawa F, Iizawa F, Ishibashi O, Kawashima H, Matsuda A, Endo N, Kawashima H. 2004. Homeobox protein MSX2 acts as a molecular defense mechanism for preventing ossification in ligament fibroblasts. Mol Cell Biol 24:3460–3472.

nature
cell biology

Regulation of endoplasmic reticulum stress response by a BBF2H7-mediated Sec23a pathway is essential for chondrogenesis

Atsushi Saito[1,5], Shin-ichiro Hino[1,5], Tomohiko Murakami[1], Soshi Kanemoto[1], Shinichi Kondo[1], Masahiro Saitoh[2], Riko Nishimura[2], Toshiyuki Yoneda[2], Tatsuya Furuichi[3], Shiro Ikegawa[3], Masahito Ikawa[4], Masaru Okabe[4] and Kazunori Imaizumi[1,6]

Many tissues have a specific signal transduction system for endoplasmic reticulum (ER) dysfunction; however, the mechanisms underlying the ER stress response in cartilage remain unclear. BBF2H7 (BBF2 human homologue on chromosome 7), an ER-resident basic leucine zipper transcription factor, is activated in response to ER stress[1] and is highly expressed in chondrocytes. In this study, we generated *Bbf2h7*$^{-/-}$ mice to assess the *in vivo* function of BBF2H7. The mice showed severe chondrodysplasia and died by suffocation shortly after birth because of an immature chest cavity. The cartilage showed a lack of typical columnar structure in the proliferating zone and a decrease in the size of the hypertrophic zone, resulting in a significant reduction of extracellular matrix proteins. Interestingly, proliferating chondrocytes showed abnormally expanded ER, containing aggregated type II collagen (Col2) and cartilage oligomeric matrix protein (COMP). We identified *Sec23a*, which encodes a coat protein complex II component responsible for protein transport from the ER to the Golgi[2,3], as a target of BBF2H7, which directly bound to a CRE-like sequence in the promoter region of *Sec23a* to activate its transcription. When Sec23a was introduced to *Bbf2h7*$^{-/-}$ chondrocytes, the impaired transport and secretion of cartilage matrix proteins was totally restored, indicating that by activating protein secretion the BBF2H7–Sec23a pathway has a crucial role in chondrogenesis. Our findings provide a new link by which ER stress is converted to signalling for the activation of ER-to-Golgi trafficking.

The ER is a critical cellular compartment in which protein folding occurs before proteins are transported to the extracellular surface or to different intracellular organelles. A number of cellular stress conditions lead to the accumulation of unfolded or misfolded proteins in the ER lumen. Eukaryotic cells can clear unfolded proteins to avoid cellular damage. This system is termed the unfolded protein response (UPR)[4,5]. ER stress transducers have important roles in UPR signal transduction. In mammalian cells, the three major transducers of the UPR are PERK (PKR-like endoplasmic reticulum kinase), IRE1 (inositol-requiring 1) and ATF6 (activating transcription factor 6). These transducers sense unfolded proteins in the ER lumen and transduce signals to the nucleus.

Recently, several new members of the CREB/ATF family that have a transmembrane domain, which allows them to associate with the ER, were identified. They are structurally similar to ATF6, and all possess a transcription-activation domain and a bZIP domain (Fig. 1a). These new members include OASIS[6,7], CREBH[8,9], AIbZIP (also known as CREB3l4 or Tisp40; refs 10, 11), Luman[12] and BBF2H7 (ref. 1). Previously, we demonstrated that BBF2H7 is cleaved at the membrane region by regulated intramembrane proteolysis (RIP) in response to ER stress, and has roles in protection from ER stress[1]. Although BBF2H7 is widely expressed in many tissues and organs, the most intense signals were detected in the proliferating zone of the cartilage in developing long bones (Fig. 1b). To assess the role of BBF2H7 *in vivo*, we generated *Bbf2h7*$^{-/-}$ mice by homologous recombination (Supplementary Information, Fig. S1). Although *Bbf2h7*$^{-/-}$ mice were generated at the expected Mendelian ratios at the embryonic stage (Supplementary Information, Fig. S1e), they had short limbs, a protruding tongue, a distended belly (Fig. 1c) and died by suffocation shortly after birth because of an immature chest cavity. Skeletal preparations showed extremely short limbs, hypoplasia of craniofacial bones and a reduction in the cartilage extracellular matrix (ECM) proteins in limbs, vertebrae and ribs (Fig. 1d). Long bones of *Bbf2h7*$^{-/-}$ mice were shorter than those of wild-type mice, although their structures were intact.

[1]Division of Molecular and Cellular Biology, Department of Anatomy, Faculty of Medicine, University of Miyazaki, 5200 Kihara, Kiyotake, Miyazaki 889-1692, Japan. [2]The Department of Molecular and Cellular Biochemistry, Graduate School of Dentistry, Osaka University, 1-8 Yamadaoka, Suita, Osaka 565-0871, Japan. [3]Laboratory for Bone and Joint Diseases, Center for Genomic Medicine, RIKEN, 4-6-1 Shirokanedai, Minato-ku, Tokyo 108-8639, Japan. [4]Genome Information Research Center and Graduate School of Pharmaceutical Sciences, Osaka University, 3-1 Yamadaoka, Suita, Osaka 565-0871, Japan.
[5]These authors contributed equally to this work.
[6]Correspondence should be addressed to K.I. (e-mail: imaizumi@med.miyazaki-u.ac.jp)

Received 2 April 2009; accepted 22 May 2009; published online 20 September 2009; DOI: 10.1038/ncb1962

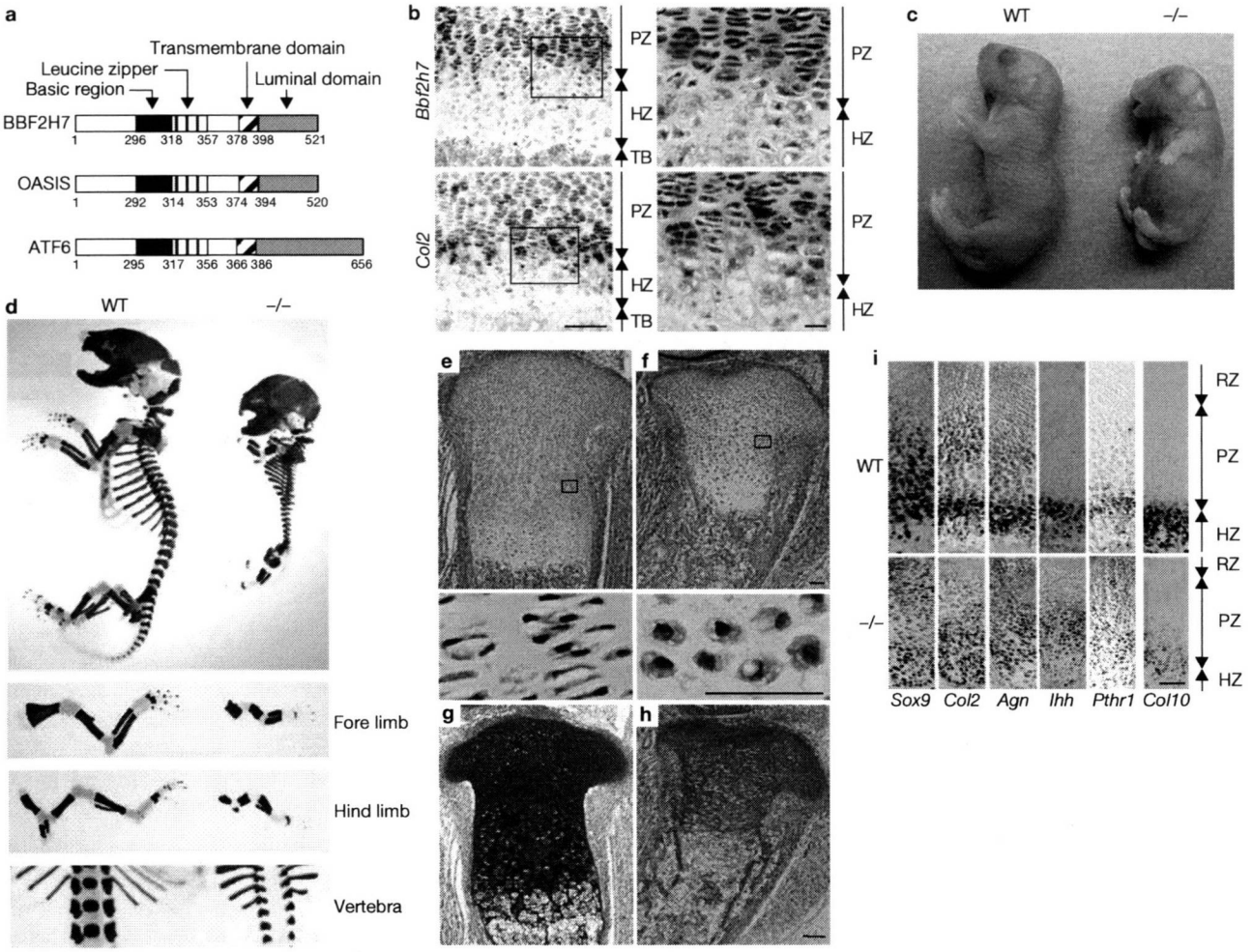

Figure 1 *Bbf2h7*$^{-/-}$ mice show severe chondrodysplasia. (**a**) Peptide features of mouse BBF2H7, OASIS and ATF6. (**b**) *In situ* hybridization for *Bbf2h7* and *Type II collagen* (*Col2*, a proliferating zone marker) in the humerus at embryonic day (E) 18.5. The right panels show higher magnification of the boxed areas in the left panels. *Bbf2h7* expression was almost restricted to the proliferating zone of the cartilage. Scale bars, 50 μm (left), 10 μm (right). (**c**, **d**) Gross morphology (**c**) and skeletal preparations stained with alcian blue and alizarin red (**d**), at E18.5. (**e**–**h**) Histology of cartilage in tibia at E18.5. Hematoxylin-eosin (HE) staining of wild-type (**e**) and *Bbf2h7*$^{-/-}$ mice (**f**). Bottom panels show higher magnifications of the boxes in **e** and **f**. Toluidine blue staining of wild-type (**g**) and *Bbf2h7*$^{-/-}$ (**h**) mice. Scale bars, 50 μm. (**i**) *In situ* hybridization for zone-specific markers in humerus at E18.5. Scale bar, 50 μm. PZ, proliferating zone; HZ, hypertrophic zone; TB, trabecular bone; RZ, resting zone; WT, wild type; –/–, *Bbf2h7*$^{-/-}$; *Agn*, *Aggrecan*; *Col10*, *type X collagen*.

Hematoxylin-eosin -stained sections of *Bbf2h7*$^{-/-}$ cartilage showed a lack of typical columnar structure in the proliferating zone with a decreased number of chondrocytes and a decrease in the size of the hypertrophic zone, although the resting zone was intact (Fig. 1e, f; Supplementary Information, Fig. S2a). In the proliferating zone of *Bbf2h7*$^{-/-}$ mice, chondrocytes showed disrupted arrangement, had a circular form and contained many vacuolar structures in the cytosol (Fig. 1e, f, bottom panels). However, these cells showed positive signals for proliferating cell nuclear antigen (PCNA) staining, indicating that chondrocytes in this zone are actually proliferating (Supplementary Information, Fig. S2b). Toluidine blue staining showed a drastic reduction of ECM proteins in the epiphyseal cartilage of *Bbf2h7*$^{-/-}$ mice compared with that of wild-type mice (Fig. 1g, h). Thus, *Bbf2h7* deficiency causes the disruption of epiphyseal cartilage, in particular, in the proliferating zone where it is associated with a significant reduction in ECM proteins.

We next examined the expression patterns of zone-specific markers[13,14] in *Bbf2h7*$^{-/-}$ mice by *in situ* hybridization (Fig. 1i). The expression levels of these markers in *Bbf2h7*$^{-/-}$ mice were almost similar to those in wild-type mice, except for that of type X collagen (*Col10*), which was significantly reduced (Fig. 1i; Supplementary Information, Fig. S2c), indicating a decrease in mature hypertrophic chondrocytes. The signals of *Ihh* and *Pthr1* were diffusely detected in the proliferating zone. Their expression patterns were different from those of wild-type mice, which were preferentially observed in the pre-hypertrophic zone. Taken together, these results indicate that the organization of the hypertrophic zone is disturbed in *Bbf2h7*$^{-/-}$ mice.

Electron microscopic analysis of wild-type mice showed proliferating chondrocytes contained well-developed, organized rough ER (Fig. 2a). In *Bbf2h7*$^{-/-}$ mice, the rough ER was abnormally expanded and included material in the lumen. Moreover, the collagen fibril network surrounding the chondrocytes was irregular and the amount of collagen was considerably reduced (Fig. 2a, bottom panels). We carried out immunohistochemistry using the proliferating zone of the humerus in *Bbf2h7*$^{-/-}$ mice. In wild-type mice, immunoreactivities of the ECM proteins Col2 (ref. 15)

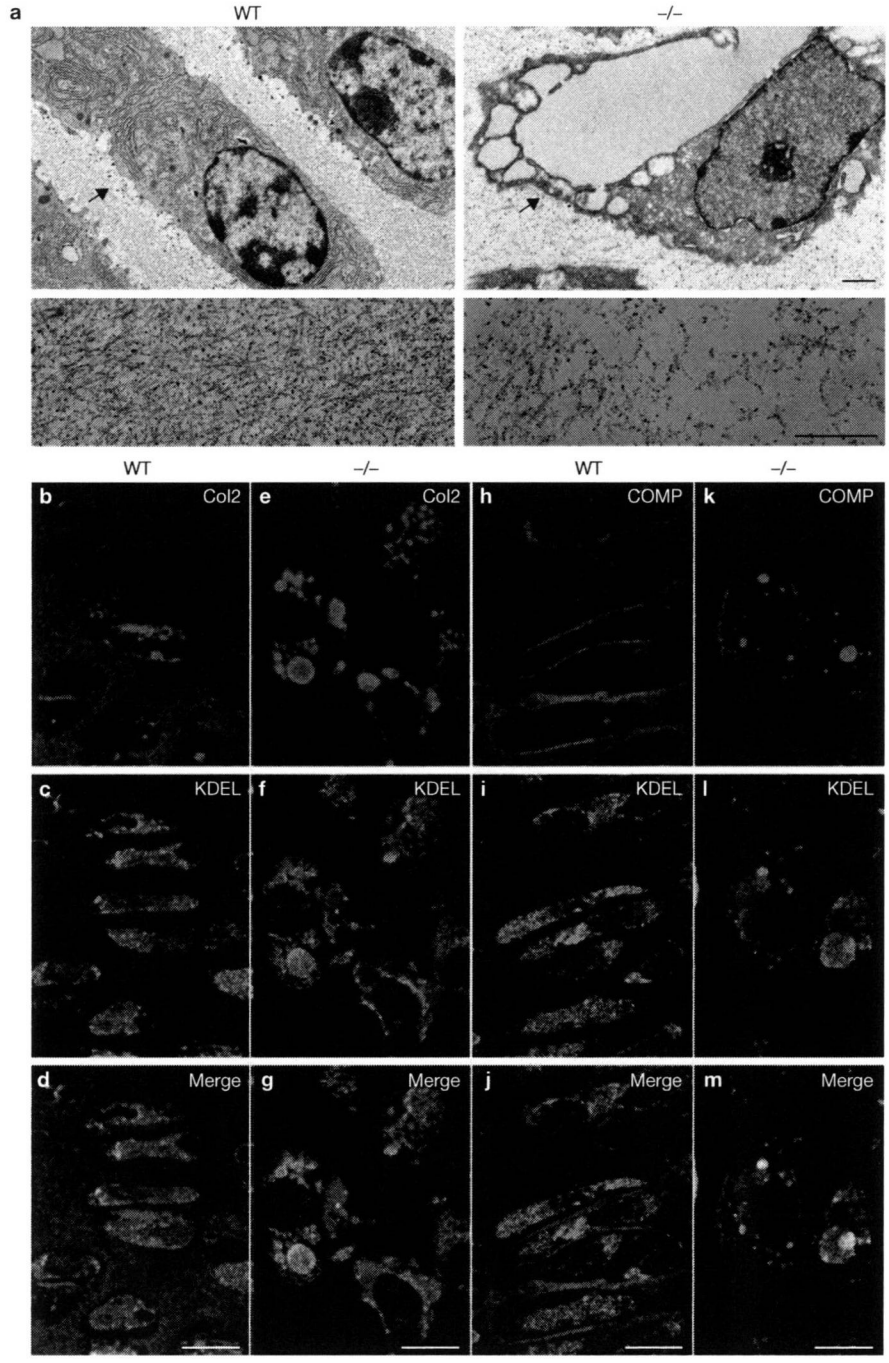

Figure 2 Col2 and cartilage oligomeric matrix protein (COMP) are accumulated in the ER lumen in *Bbf2h7*-deficient mice. (**a**) Electron microscopy images of proliferating chondrocytes (top) and cartilage matrix of the proliferating zone (bottom) of humerus at E18.5. Arrows show rough ER. In *Bbf2h7*$^{-/-}$ mice, the rough ER was abnormally expanded and included material in the lumen. Scale bars, 1 μm. (**b**–**m**) Immunohistochemistry analysis of Col2 and COMP in the proliferating zone in humerus at E18.5. KDEL is an ER marker. Note that Col2 and COMP are accumulated within cells, and are scarcely detected in the extracellular space, in *Bbf2h7*$^{-/-}$ mice. Scale bars, 10 μm. WT, wild type; –/–, *Bbf2h7*$^{-/-}$.

and COMP[16] were mainly observed in the extracellular space of chondrocytes (Fig. 2b, h). In contrast, in *Bbf2h7*$^{-/-}$ mice, these immunoreactivities were scarcely detected in the extracellular space, but were accumulated in the intracellular space, appearing as differently sized aggregates (Fig. 2e, k). Double staining with KDEL, an ER marker, showed that the aggregates of Col2 and COMP were accumulated in the ER (Fig. 2g, m), indicating that secretion of ECM proteins from chondrocytes in the proliferating zone is prevented in *Bbf2h7*$^{-/-}$ mice, and that this defect in protein secretion could lead to the disruption of the ECM network in cartilage, and of cartilage zone formation. Morphological changes in other tissues, including pancreatic beta cells, could not be detected in *Bbf2h7*$^{-/-}$ mice at the embryonic stage (Supplementary Information, Fig. S3).

We further investigated the effects of *Bbf2h7* deficiency on the formation of epiphyseal cartilage using micromass culture of mesenchymal cells

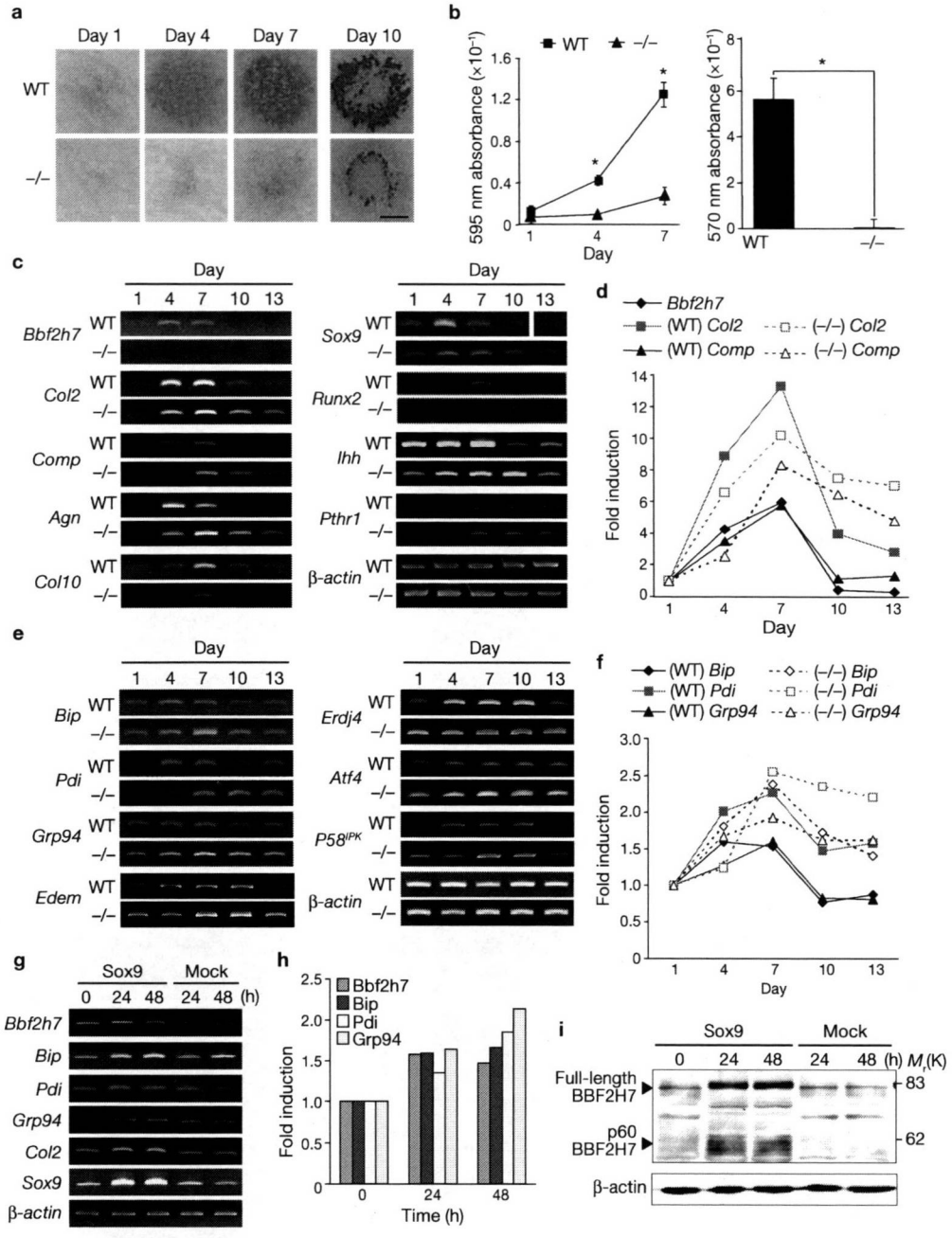

Figure 3 Expression of chondrocyte differentiation markers and ER stress-related genes in cultured cells. (**a**–**f**) Mesenchymal cells were maintained as micromass cultures for the number of days indicated. (**a**) Cells were stained with alcian blue (for cartilage matrix proteins) and alizarin red (for mineralization). *Bbf2h7*$^{-/-}$ cells showed significantly lower extracellular matrix (ECM) protein secretion and mineralization than wild-type cells. Scale bar, 1 mm. (**b**) Quantification of absorbance from cells stained with alcian blue (left) and alizarin red (right). Data are mean ± s.d., $n = 5$, $^{*}P < 0.001$ (Student's *t*-test). (**c**) RT-PCR analysis of chondrocyte differentiation markers in micromass cultures. In *Bbf2h7*$^{-/-}$ cells, the expression of these markers was continued until the late phase of the culture. The samples of *Sox9* were run as part of the same experiment on the same gel. (**d**) Quantitative analysis of *Bbf2h7*, *Col2* and *Comp* mRNA expression. (**e**) RT-PCR analysis of ER stress-related genes in micromass culture. Mild ER stress was transiently induced in chondrocytes during their differentiation. In *Bbf2h7*$^{-/-}$ cells, ER stress was increased compared with that in wild-type cells, and the induction was prolonged until day 13 of the culture. (**f**) Quantitative analysis of *Bip*, *Pdi* and *Grp94* mRNA expression. (**g**–**i**) Expression of ER stress-related genes in primary cultured chondrocytes infected with an adenovirus expressing Sox9 or an empty vector (Mock), as determined by RT-PCR (**g**) and western blotting (**i**) . Note that *Bbf2h7*, *Bip*, *Pdi* and *Grp94* were slightly upregulated and the active, amino-terminal form of BBF2H7 (p60 BBF2H7) was generated by Sox9. (**h**) Quantitative analysis of *Bbf2h7*, *Bip*, *Pdi* and *Grp94* mRNA expression. WT, wild type; –/–, *Bbf2h7*$^{-/-}$; Mock, empty vector.

prepared at embryonic day (E) 11.5. Alcian blue and alizarin red stainings in *Bbf2h7*$^{-/-}$ cells were much weaker than those in wild-type cells, at each time point (Fig. 3a, b). Expression of *Bbf2h7* mRNA showed an induction peak that was maintained from day 4 to 7 of the culture (Fig. 3c, d). In *Bbf2h7*$^{-/-}$ cells, expression of *Col2*, *Comp*, *Agn*, *Sox9*, *Runx2*, *Ihh* and *Pthr1* continued until a late phase of the culture, although expression levels were almost equal to those in wild-type cells (Fig. 3c, d), indicating that chondrocyte differentiation is delayed and that this involves

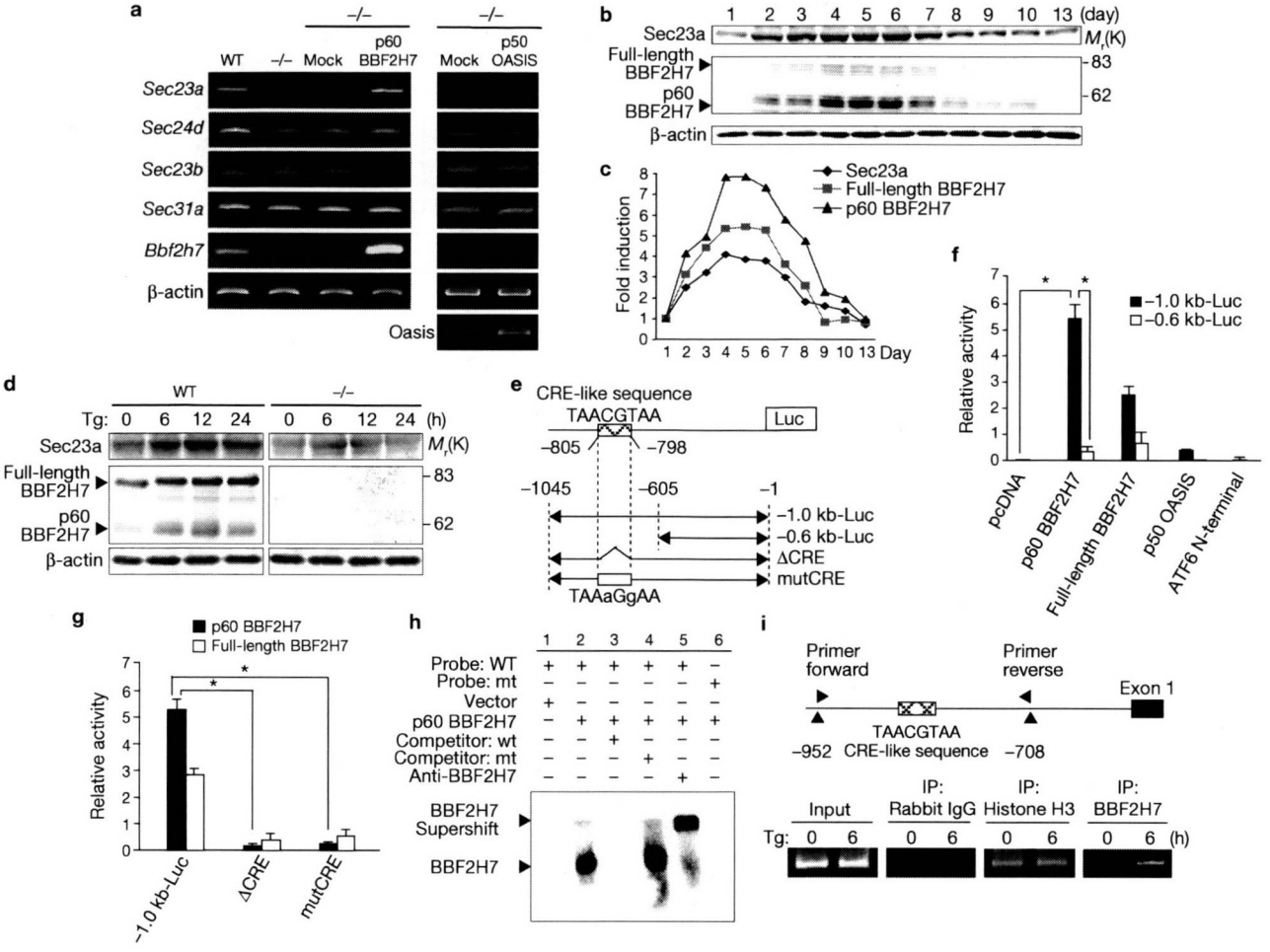

Figure 4 *Sec23a* is a target of BBF2H7. (**a**) RT-PCR analysis using primary cultured chondrocytes. Introduction of p60 BBF2H7 into *Bbf2h7*$^{-/-}$ chondrocytes rescued *Sec23a* expression. Note that OASIS, which is a transcription factor and has a similar structure to BBF2H7, could not rescue *Sec23a* expression. (**b**) Western blotting analysis of Sec23a in mesenchymal cells maintained as a micromass culture. Note that expression of Sec23a proteins at the indicated time points was synchronized with that of BBF2H7. (**c**) Quantitative analysis of Sec23a, full-length BBF2H7 and p60 BBF2H7 protein expression. (**d**) Western blotting analysis using lysates extracted from wild-type (left) and *Bbf2h7*$^{-/-}$ (right) primary cultured chondrocytes exposed to thapsigargin (1 μM; an ER stressor). (**e**) The mouse Sec23a promoter region and reporter plasmids. (**f**) Reporter assays using full-length 1.0-kb and 0.6-kb *Sec23a* promoters. ATDC5 cells were transfected with the indicated constructs and the reporter plasmid pGL3-*Sec23a* promoter (1.0-kb or 0.6-kb) attached to a luciferase gene. The relative luciferase activities in the cells were determined. Data are mean ± s.d., $n = 5$, $^*P < 0.001$(Student's *t*-test). (**g**) Reporter assays of ΔCRE and mutCRE using ATDC5 cells (mean ± s.d., $n = 3$, $^*P < 0.001$(student's *t*-test). (**h**) Gel shift assay shows that the binding of p60 BBF2H7 and the CRE-like sequence was abolished by a competitor (lane 3), and a supershift by an anti-BBF2H7 antibody (lane 5) was detected. (**i**) Chromatin immunoprecipitation assay using primary cultured chondrocytes treated with thapsigargin (1 μM). Top panel, schematic representation of the mouse *Sec23a* promoter and the primer sites. Bottom panel, immunoprecipitation of chromatin with the indicated antibodies. Tg, thapsigargin; Luc, luciferase gene; mt, mutant; IP, immunoprecipitate; WT, wild type; -/-, *Bbf2h7*$^{-/-}$; Mock, empty vector.

reduced secretion of cartilage ECM proteins in *Bbf2h7*$^{-/-}$ cells. The results were consistent with *in vivo* findings from the epiphyseal cartilage in *Bbf2h7*$^{-/-}$ mice. Chondrocyte differentiation requires the attachment of chondrocytes to Col2, in developing bone[17,18]. Thus, pertubation of normal chondrocyte differentiation and cartilage zone formation could be caused by decreased secretion of ECM proteins in *Bbf2h7*$^{-/-}$ mice.

All the ER stress-related genes that we examined were slightly upregulated at days 4 and 7 in micromass culture of wild-type cells (Fig. 3e, f), and chaperone molecules, BiP, PDI and GRP94, were also upregulated (data not shown), indicating that mild ER stress is transiently induced in chondrocytes during their normal differentiation. The expression of ER stress-regulated genes and chaperone molecules in *Bbf2h7*$^{-/-}$ cells was increased compared with that in wild-type cells, and the induction was prolonged until day 13. In the rib cartilage, expression of the ER stress-related genes was also higher in *Bbf2h7*$^{-/-}$ than in wild-type mice (Supplementary Information, Fig. S4). Thus, *Bbf2h7* deficiency causes severe ER stress in chondrocytes, which could be induced by the accumulation of ECM proteins in the ER lumen.

Sox9, which is essential for chondrocyte differentiation[14,19], was highly expressed at days 4 and 7 in the micromass culture (Fig. 3c). *Sox9* expression at these time points could facilitate synthesis of various proteins for chondrocyte differentiation and could induce ER stress in chondrocytes. Reverse transcription (RT)-PCR showed that *Bbf2h7*, *Bip*, *Pdi* and *Grp94* were slightly, but significantly, upregulated by Sox9 (Fig. 3g, h). An active form of BBF2H7, p60 BBF2H7, was obtained

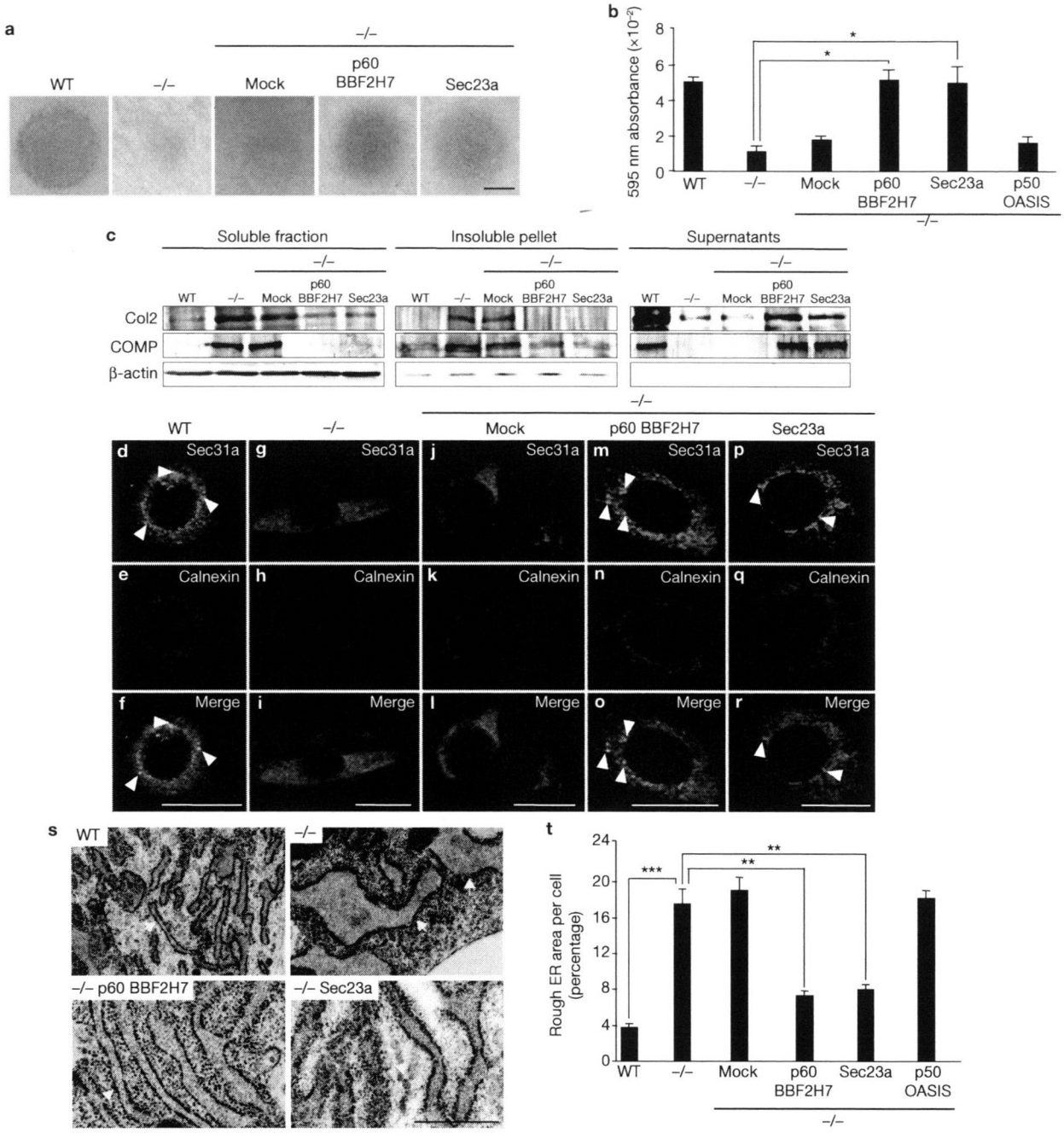

Figure 5 The introduction of Sec23a in *Bbf2h7*$^{-/-}$ cells improves secretion of ECM proteins. (**a**) Mesenchymal cells prepared from wild-type and *Bbf2h7*$^{-/-}$ mice were maintained as micromass cultures for four days, and stained with alcian blue. Infection of *Bbf2h7*$^{-/-}$ cells with an adenovirus expressing p60 BBF2H7 or Sec23a improved the secretion of ECM proteins. Scale bar, 1 mm. (**b**) Quantification of absorbance from cells stained by alcian blue. The introduction of OASIS could not rescue the secretion of ECM proteins in *Bbf2h7*$^{-/-}$ cells. Data are mean ± s.d. $n = 5$, except for *Bbf2h7*$^{-/-}$ *p50* OASIS $n = 3$, $^{*}P < 0.001$ Student's *t*-test. (**c**) Western blotting of Col2 and COMP using lysates extracted from primary cultured chondrocytes in wild-type and *Bbf2h7*$^{-/-}$ mice. Note that the lack of intracellular accumulation of Col2 and COMP, which are secreted into the media by introduction of p60 BBF2H7 or Sec23a into the chondrocytes. (**d**–**r**) Double-immunofluorescence of Sec31a and calnexin (an ER marker) in primary cultured chondrocytes of wild-type and *Bbf2h7*$^{-/-}$ mice. Arrowheads show punctates of Sec31a recruited to the ER exit site. Scale bars, 20 μm. (**s**) Electron microscopic images of primary cultured chondrocytes from wild-type and *Bbf2h7*$^{-/-}$ mice. Arrows show rough ER. Note disordered parallel stacks of flattened cisternae in *Bbf2h7*$^{-/-}$ chondrocytes infected with Sec23a. Scale bars, 0.5 μm. (**t**) Two-dimensional analysis of rough ER area using electron micrographs. The introduction of OASIS could not improve the size of the rough ER in *Bbf2h7*$^{-/-}$ chondrocytes. Mean ± s.d., $n = 20$, except for *Bbf2h7*$^{-/-}$ OASIS $n = 5$; $^{**}P < 0.05$, $^{***}P < 0.01$ (Student's *t*-test). WT, wild type; −/−, *Bbf2h7*$^{-/-}$; Mock, empty vector.

in response to *Sox9* expression by western blotting analysis (Fig. 3i). Therefore, *Sox9* could induce mild ER stress and activate BBF2H7 during chondrocyte differentiation.

We compared gene expressions in primary cultured chondrocytes prepared from the rib cartilage of wild-type and *Bbf2h7*$^{-/-}$ mice at E18.5 using a microarray. Various genes associated with the protein secretory

pathway and ER biogenesis were significantly downregulated in *Bbf2h7*$^{-/-}$ chondrocytes (Supplementary Information, Fig. S5a). Among these genes, which are directly or indirectly controlled by BBF2H7, *Sec23a* was the most downregulated. RT-PCR showed that *Sec23a* was 80% downregulated, but the expression of the other genes encoding components of the COPII vesicle was not changed (Fig. 4a). Western blotting (Supplementary Information, Fig. S5b) and immunofluorescence (Supplementary Information, Fig. S5c) also showed that Sec23a is significantly decreased in *Bbf2h7*$^{-/-}$ chondrocytes. We infected primary cultured chondrocytes prepared from *Bbf2h7*$^{-/-}$ mice with an adenovirus expressing p60 BBF2H7. *Sec23a* was significantly upregulated by overexpression of p60 BBF2H7, but expression of the other genes, including components of the COPII vesicle, were not affected (Fig. 4a; Supplementary Information, Fig. S5d). An active form of OASIS (p50 OASIS), which is structurally very similar to BBF2H7 and is expressed in osteoblasts and astrocytes[6], could not induce *Sec23a* expression, indicating that *Sec23a* induction by BBF2H7 is specific.

In a micromass culture at day 1, *Sec23a* expression was relatively low (Fig. 4b, c). This signal markedly increased from day 2 to 6, before decreasing. The expression pattern of *Sec23a* was very similar to that of *BBF2H7* (Fig. 4b, c). As BBF2H7 is activated in response to ER stress[1], if *Sec23a* is a direct target of BBF2H7, *Sec23a* should be induced in chondrocytes undergoing ER stress. Indeed, in primary cultured chondrocytes of wild-type mice, *Sec23a* was markedly induced during ER stress, which was synchronized with the activation of BBF2H7 (Fig. 4d). In contrast, the induction of *Sec23a* was significantly attenuated in *Bbf2h7*$^{-/-}$ chondrocytes. These findings strongly indicate that *Sec23a* is a direct target of BBF2H7.

To identify the cis-acting element in the *Sec23a* promoter region that is responsive to BBF2H7, we searched within 2-kb upstream of the *Sec23a* transcription start site, using the TFSEARCH (http://mbs.cbrc.jp/research/db/TFSEARCH.html). We found a CRE (cAMP-responsive element)-like sequence (5′-TAACGTAA-3′, −805 to −798 base pairs) that is conserved among human, mouse and rat. We previously reported that BBF2H7 can bind to CRE (5′-TGACGTTT-3′) and promote transcription[1]. We performed reporter assays using a reporter gene carrying a 1-kb and a 0.6-kb promoter region of *Sec23a* (Fig. 4e). In cells transfected with a 1-kb reporter construct, reporter activity was significantly induced by introduction of an expression vector for full-length BBF2H7 or p60 BBF2H7 (Fig. 4f). However, reporter activity was rarely induced by BBF2H7 in cells transfected with a 0.6-kb reporter construct. Moreover, reporter activity in cells transfected with 1.0-kb *Sec23a* promoter region lacking, or containing a mutated, CRE-like sequence (ΔCRE and mutCRE, respectively) was dramatically reduced (Fig. 4g).

To confirm that BBF2H7 directly binds to the CRE-like sequence, we performed electrophoretic mobility shift assays (EMSAs). p60 BBF2H7 bound to the CRE-like sequence (Fig. 4h). This binding was abolished by incubation with a 100-fold excess of unlabelled competitors, but not by mutated competitors. The addition of an anti-BBF2H7 antibody caused a supershift (Fig. 4h). Furthermore, we carried out a chromatin immunoprecipitation (ChIP) assay (Fig. 4i). A high level of BBF2H7 binding to the endogenous *Sec23a* promoter was detected in chondrocytes exposed to ER stress. We conclude that BBF2H7 directly binds to the CRE-like sequence within the *Sec23a* promoter region and facilitates its transcription, in chondrocytes.

Sec23a has crucial roles in COPII vesicle formation and anterograde transport of cargo proteins from the ER to the Golgi[3]. Therefore, abnormal cartilage formation involving disturbed secretion of ECM proteins and aggregation of Col2 and COMP in the ER lumen in *Bbf2h7*$^{-/-}$ mice could be associated with decreased *Sec23a* expression, in chondrocytes. In micromass-cultured *Bbf2h7*$^{-/-}$ cells infected with an adenovirus expressing p60 BBF2H7 or Sec23a, secretion of ECM proteins significantly increased and alcian blue ECM-positive contents recovered to the level of those in wild-type cells (Fig. 5a, b). In primary cultured *Bbf2h7*$^{-/-}$ chondrocytes infected with p60 BBF2H7 or Sec23a, the intracellular accumulation of Col2 and COMP completely ceased, and these ECM proteins were secreted into the media as with wild-type chondrocytes (Fig. 5c).

Sec23a recruits other components of the COPII vesicle, including Sec31, and completes the complex before transporting secretory proteins from the ER to the Golgi[2,3]. A mutation of *Sec23a* causes cranio-lenticulo-sutural dysplasia (CLSD), which is characterized by a malformed craniofacial structure involving chondrodysplasia, and cataracts[20]. The mutation reduces the affinity of the Sec13–Sec31 complex[20]. Hence, we examined the localization of Sec31 in primary cultured chondrocytes of *Bbf2h7*$^{-/-}$ mice. Sec31a showed a punctate localization surrounding the ER, which is assumed to recruit to the exit site of the ER membrane in wild-type chondrocytes (Fig. 5d, f). In *Bbf2h7*$^{-/-}$ chondrocytes, Sec31a was diffusely localized in the cytosol and the punctate localization surrounding the ER was not observed (Fig. 5g, i). This mislocalization of Sec31a was rescued by the overexpression of p60 BBF2H7 (Fig. 5m, o) or Sec23a (Fig. 5p, r).

In addition to the disturbance of ECM protein secretion, drastic expansion of the rough ER was observed in *Bbf2h7*$^{-/-}$ chondrocytes (Fig. 2a). We examined ultrastructural changes of rough ER in *Bbf2h7*$^{-/-}$ chondrocytes infected with p60 BBF2H7 or Sec23a (Fig. 5s). The two-dimensional size of the rough ER in *Bbf2h7*$^{-/-}$ chondrocytes infected with p60 BBF2H7 or Sec23a was obtained (Fig. 5s,t). However, *Bbf2h7*$^{-/-}$ chondrocytes infected with Sec23a showed disordered parallel stacks of flattened cisternae that were not completely rescued, this was in contrast to the effect of p60 BBF2H7 introduction. As shown in the microarray data, many other genes, including ER biogenesis-related genes, are also under BBF2H7 control. Therefore, those genes could also be necessary for the complete rescue of *Bbf2h7*$^{-/-}$ chondrocytes. Taken together, these results indicate that perturbance of ER to Golgi trafficking and reduced secretion of ECM proteins are directly due to *Bbf2h7* deficiency and that a BBF2H7-mediated Sec23a pathway is essential for the ER stress-coupled vesicle transport system in chondrocytes.

Sec23b, which is paralogous to Sec23a, functions commutatively with Sec23a to prevent disruption of the secretory pathway. The localization of Sec23b in tissue is different from that of Sec23a[21]. The expression level of Sec23b in chondrocytes is very low; it is much higher in fibroblasts (Supplementary Information, Fig. S6a). In *Bbf2h7*$^{-/-}$ fibroblasts, the ER showed only a slight expansion of its lumen (Supplementary Information, Fig. S6b). Therefore, Sec23b is presumed to be sufficient to compensate for the downregulation of Sec23a in *Bbf2h7*$^{-/-}$ fibroblasts. The severe pathology in the cartilage of *Bbf2h7*$^{-/-}$ mice could be explained by insufficient availability of Sec23b to provide normal Sec23 function.

ER stress markers are mildly upregulated during chondrocyte differentiation in micromass cultures and primary cultures of chondrocytes. Moreover, BBF2H7 is highly cleaved at its membrane region in response to stimulation of differentiation by Sox9, indicating that ER stress is induced during normal chondrocyte differentiation.